**US Army Corps
of Engineers**
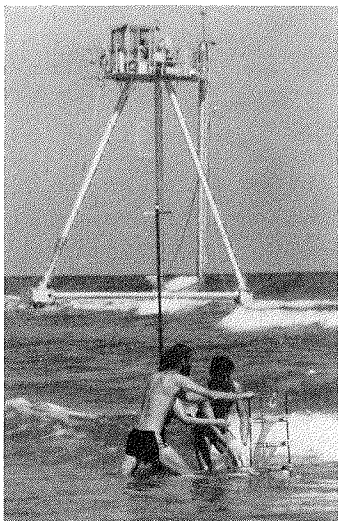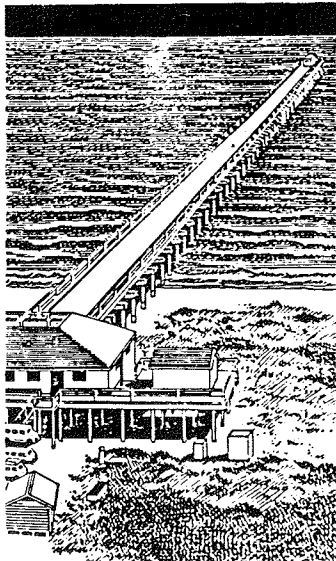
SUPERDUCK SURF ZONE SAND TRANSPORT EXPERIMENT

by

Julie Dean Rosati, Kathryn J. Gingerich, Nicholas C. Kraus

Coastal Engineering Research Center

DEPARTMENT OF THE ARMY
Waterways Experiment Station, Corps of Engineers
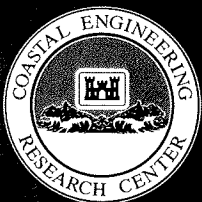3909 Halls Ferry Road, Vicksburg, Mississippi   39180-6199

REPORT DOCUMENTATION PAGE

Form Approved
OMB No. 0704-0188

1a. REPORT SECURITY CLASSIFICATION			1b. RESTRICTIVE MARKINGS			
Unclassified						

2a. SECURITY CLASSIFICATION AUTHORITY	3. DISTRIBUTION / AVAILABILITY OF REPORT
	Approved for public release; distribution unlimited
2b. DECLASSIFICATION / DOWNGRADING SCHEDULE	

4. PERFORMING ORGANIZATION REPORT NUMBER(S)	5. MONITORING ORGANIZATION REPORT NUMBER(S)
Technical Report CERC-90-10	

6a. NAME OF PERFORMING ORGANIZATION USAEWES, Coastal Engineering Research Center	6b. OFFICE SYMBOL (If applicable)	7a. NAME OF MONITORING ORGANIZATION

6c. ADDRESS (City, State, and ZIP Code)	7b. ADDRESS (City, State, and ZIP Code)
3909 Halls Ferry Road Vicksburg, MS 39180-6199	

8a. NAME OF FUNDING / SPONSORING ORGANIZATION US Army Corps of Engineers	8b. OFFICE SYMBOL (If applicable)	9. PROCUREMENT INSTRUMENT IDENTIFICATION NUMBER

8c. ADDRESS (City, State, and ZIP Code)	10. SOURCE OF FUNDING NUMBERS			
	PROGRAM ELEMENT NO.	PROJECT NO.	TASK NO.	WORK UNIT ACCESSION NO.
Washington, DC 20314-1000				34321

11. TITLE (Include Security Classification)

SUPERDUCK Surf Zone Sand Transport Experiment

12. PERSONAL AUTHOR(S)
Rosati, Julie Dean; Gingerich, Kathryn J.; Kraus, Nicholas C.

13a. TYPE OF REPORT	13b. TIME COVERED	14. DATE OF REPORT (Year, Month, Day)	15. PAGE COUNT
Final report	FROM _____ TO _____	July 1990	76

16. SUPPLEMENTARY NOTATION
Available from National Technical Information Service, 5285 Port Royal Road, Springfield, VA 22161

17.	COSATI CODES		18. SUBJECT TERMS (Continue on reverse if necessary and identify by block number)
FIELD	GROUP	SUB-GROUP	Field experiment SUPERDUCK experiment, Duck, NC
			Longshore sand transport Surf zone
			Streamer trap

19. ABSTRACT (Continue on reverse if necessary and identify by block number)

   The procedures and results of an experiment performed to measure the longshore sand transport rate in the surf zone as part of the SUPERDUCK field data collection project are described in this report. Cross-shore distributions of the longshore sand transport rate, as well as its variation at a point in the surf zone through time, were measured with portable sand traps. Comparison of measurements made with two closely spaced traps indicates trap reliability and consistency. The longshore sand transport rate measured at SUPERDUCK was found to be closely related to the product of wave height and longshore current speed, consistent with previously derived theoretical models of transport. The correlation was considerably improved, however, by including corrections due to energy dissipation introduced by breaking waves and the variation in the longshore current speed. A complete listing of the sand transport rate, wave height, longshore current, and sand grain size data is given.

20. DISTRIBUTION / AVAILABILITY OF ABSTRACT	21. ABSTRACT SECURITY CLASSIFICATION	
☒ UNCLASSIFIED/UNLIMITED ☐ SAME AS RPT. ☐ DTIC USERS	Unclassified	
22a. NAME OF RESPONSIBLE INDIVIDUAL	22b. TELEPHONE (Include Area Code)	22c. OFFICE SYMBOL

DD Form 1473, JUN 86   *Previous editions are obsolete.*   SECURITY CLASSIFICATION OF THIS PAGE

PREFACE

The investigation described in this report was authorized as part
of the Civil Works Research and Development Program by Headquarters, US Army
Corps of Engineers (HQUSACE). This study was conducted under the Shore
Protection and Restoration Program, Surf Zone Sediment Transport Processes
Work Unit 34321, at the Coastal Engineering Research Center (CERC) of the US
Army Engineer Waterways Experiment Station (WES). Messrs. John H. Lockhart,
Jr., and John G. Housley were HQUSACE Technical Monitors.

The study was performed by CERC in two phases: a field experiment
planned and conducted from 1 June 1986 through 30 September 1986, and subse-
quent analysis of the data conducted from 1 October 1986 to 30 September 1989.
Dr. Nicholas C. Kraus, Senior Scientist, Research Division (RD), CERC, was
Principal Investigator (PI) of Work Unit 34321 during the first phase of the
study; Ms. Kathryn J. Gingerich, Coastal Processes Branch (CPB), RD, was PI
during the second phase of the study; and Ms. Julie Dean Rosati, CPB, was PI
during preparation of this report.

Key members who assisted in the data collection, their affiliations at
the time of the project, and their major function during data collection were
Dr. Lindsay Nakashima, Louisiana Geological Survey, sediment processing,
surveying, and experiment design; Messrs. Gary L. Howell and C. Ray Townsend,
Prototype Measurement and Analysis Branch, CERC, current meter setup and
current measurement; Ms. Jane M. Smith, Oceanography Branch (OB), RD, current
data collection and trap operator; Ms. Mary A. Cialone, CPB, surveying,
sediment processing, and trap operator; Dr. Shintaro Hotta, Tokyo Metropolitan
University, Tokyo, Japan, photopole wave measurement team leader; Mr. Bruce A.
Ebersole, CPB, and Dr. Steven A. Hughes, OB, photopole camera operators and
trap operators. Field assistants were Drs. Hans Hanson and Magnus Larson,
University of Lund, Sweden; Mr. Jack Kooistra, Queens University, Canada; Mr.
Pascal Collotte, France; Ms. Tamsen S. Dozier, Estuarine Engineering Branch,
Hydraulics Laboratory, WES; Messrs. Paul Bowen, Myles Pocta, and Jerry Swean,
US Army Engineer (USAE) District, Norfolk; Mr. Ted Bales and Ms. Trill
Rulison, USAE District, Alaska; Messrs. Rick Champion and John Miller, USAE
District, Mobile; Ms. Lynn Koeth Bocamazo and Mr. Joe Vietri, USAE District,

1

CONTENTS

3

LIST OF TABLES

LIST OF FIGURES

SUPERDUCK SURF ZONE SAND TRANSPORT EXPERIMENT

PART I: INTRODUCTION

Purpose and Scope of Report

1.   This report describes procedures and results of field data collection projects performed to measure the longshore sand transport rate in the surf zone as a part of the SUPERDUCK field data collection project.   The experiments described herein were conducted from 11 to 23 September 1986. Certain introductory sections of this report have been taken directly from a companion report by Kraus, Gingerich, and Rosati (1989), who describe the DUCK85 field data collection project.   The objective of these sand transport experiments was to measure synoptically the longshore sand transport rate together with the physical factors that produce and control the sand movement, including local waves, longshore current, water level, and nearshore bathymetry.   A range of wave and current conditions occurred during the SUPERDUCK data collection, resulting in an extensive data set on temporal variations in the longshore sand transport rate at points in the surf zone and vertical distributions through the water column.

2.   This report is intended to provide complete documentation of the SUPERDUCK surf zone sand transport experiment, including a compilation of the data.   Information is given on experiment equipment and methodology to allow critical examination of techniques used.   Data given include transport rates, current speeds, wave heights and periods, grain size distributions, water levels, and arrangement of the experiments.   Supplementary data on meteorology and offshore wave conditions are given, and reference is made to sources of more complete information.

Background

3.   Estimates of the longshore sand transport rate are required in a multitude of projects involving shore protection, beach nourishment, and harbor and navigation channel maintenance.   In addition, during the past decade considerable progress has been made in numerical modeling of nearshore

waves, currents, and beach change. Beach morphology response models are moving from the research level to the practical level as engineering design tools. A requirement in making this transition is improved capability for predicting the longshore sand transport rate, not only the total longshore transport rate but also its distribution across the surf zone, through the water column and its variation with time. For example, these distributions are needed for estimating bypassing around, over, and through groins and jetties and behind detached breakwaters.

4. Presently available predictive formulas for the longshore sand transport rate are generally acknowledged as providing only a rough approximation of the actual rate. The number of accepted field measurements comprising the data base is surprisingly small considering the importance of the problem, and scatter in the data is great, reflecting randomness in the physical processes, limitations in measurement techniques, and simplifications in predictive expressions used to describe fluid and sand motion. Presently employed predictive formulas for the transport rate do not incorporate dependencies on grain size, breaking wave type or wave-induced turbulence, properties of the waves or longshore current beyond mean values, or influence of the local bottom shape. The transport rate is expected to greatly depend on location in the surf zone, and its dependency on local conditions must be known to calculate cross-shore and vertical distributions.

5. Recognizing the need for point measurements of the longshore sand transport rate to obtain cross-shore and vertical distributions, the Surf Zone Sediment Transport Processes Research Work Unit was begun in 1985. This work unit, under the Shore Protection and Restoration Program at the Coastal Engineering Research Center (CERC) of the US Army Engineer Waterways Experiment Station, initiated a series of field experiments aimed at collecting comprehensive data sets on sand transport and processes responsible for the sand movement. Field data collection was planned for beaches composed of different materials ranging from fine sand to gravel and for wave climates ranging from small to large wave steepness. This report describes the results of the SUPERDUCK experiment, the second field data collection project in the planned series.

6

Sand Transport Measurement Methods

6. In preparation for the first field data collection project, DUCK85, Kraus (1987) surveyed available sand transport measurement methods (tracer, impoundment, and traps) and concluded that traps offered the best means to obtain transport rate data compatible with the accuracy and detail required by existing numerical models which simulate beach evolution. Traps were also determined to be the least expensive of the three methods.

7. Portable traps allow measurement of the vertical distribution of the transport rate (transport at the bed and through the water column), and simultaneous deployment of traps at intervals across the surf zone enables measurement of the cross-shore distribution of the longshore transport rate. Traps can also be repeatedly deployed at one or two points in the surf zone to obtain temporal variations of the sand transport rate. Traps measure the sand flux, a quantity directly related to the transport rate, and not simply a sediment concentration. As in concentration measurements, transported particles are automatically retained by the traps and made available for analysis. Traps collect the material that actually moves, including sand, shell fragments, and other particles of size nominally larger than the trap mesh, and no assumptions need be made about grain size, as required in tracer studies. Mean wave and current conditions in the surf zone typically change on the order of minutes, and traps are well suited to such a sampling interval as opposed to tracer and impoundment methods. Traps are also inexpensive to construct and maintain, and only a minimum amount of training is necessary to use them. Disadvantages of traps include the potential for scour and, in surf zones, restriction to use with significant breaking wave heights on the order of 1 m or less.

SUPERDUCK Field Data Collection Project

8. During September and October 1986, CERC hosted and participated in a major multidisciplinary and multi-institutional nearshore processes field data collection project called SUPERDUCK. The name SUPERDUCK derives from the location of CERC's Field Research Facility (FRF), the site of the experiment, which is located near the village of Duck, North Carolina, on the Outer Banks

barrier islands (Figure 1). More than 50 researchers from CERC, other Govern-
ment agencies, universities, and organizations from overseas participated in
SUPERDUCK to conduct a wide variety of nearshore process investigations.

9. Patterned after the DUCK85 experiment, the SUPERDUCK project
consisted of two parts: a September phase that took advantage of relatively
low wave heights to perform labor-intensive experiments in the surf zone and
an October phase that used primarily electronic instrumentation and remote
sensing to measure storm-related nearshore processes. The surf zone sand
transport data collection was performed in September as a self-contained
program by CERC researchers with interest in measuring surf zone waves,
currents, and sand transport.
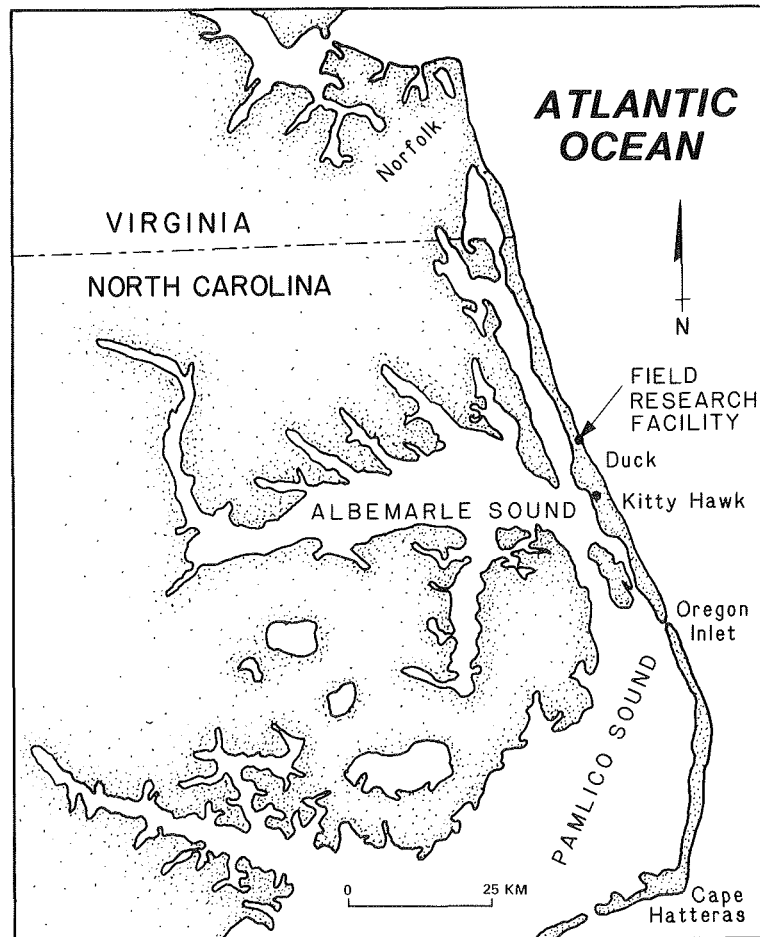
Figure 1. Location map for the FRF

8

10. The CERC surf zone data collection effort benefitted from the extended coverage provided by experiments performed concurrently by other research teams, yielding data on beach profiles, offshore waves and currents, and wind. Reports describing results of SUPERDUCK experiments related to the work discussed here include: Birkemeier et al. (1989), a report describing instruments used and data collected at the FRF during both the September and October phases of the SUPERDUCK data collection project; Crowson et al. (1988), a summary report of the 30 different experiments conducted during both phases of SUPERDUCK; Ebersole and Hughes (in preparation), a companion data report describing the surf zone wave measurement method and results, conducted during the September phase; Stauble et al. (in preparation), a report discussing beach foreshore sediment and dynamics during the October phase of SUPER-DUCK; Byrnes (1989), a data summary report of sediment characteristics during the October phase of SUPERDUCK; and Kraus, Gingerich, and Rosati (1988), revised values of the DUCK85 total transport rates and discussion of results from SUPERDUCK. Additional data are compiled in an FRF summary data report for September 1986 (FRF 1986). A video documenting the SUPERDUCK experiments was also produced (Hughes, Kraus, and Richardson 1987).

Report Contents

11. An orientation to the study site and description of the experiment equipment, methodology, and analysis procedures are given in Part II. Selected results and characteristics of the data are presented in Part III, and a general evaluation of the field project is given in Part IV. Appendix A contains a listing of the data and explanatory discussion, and Appendix B lists the notation used in this report.

PART II: BACKGROUND OF THE EXPERIMENT

Experiment Site

12. Data collection activities were coordinated from a base camp estab-
lished on the beach near the north property line of the FRF. Figure 2
provides a plan-view sketch of the base camp, FRF coordinate system, and the
general physical arrangement of a typical data collection run (bathymetry
measured on 23 September 1986). The area near the north property line was
selected to avoid possible interference of waves, currents, and nearshore
topography in the vicinity of the experiments with the 600-m-long FRF pier
located approximately 950 m to the south. An air-conditioned trailer located
behind the duneline provided a protected environment for data recorders and
other sensitive instruments.
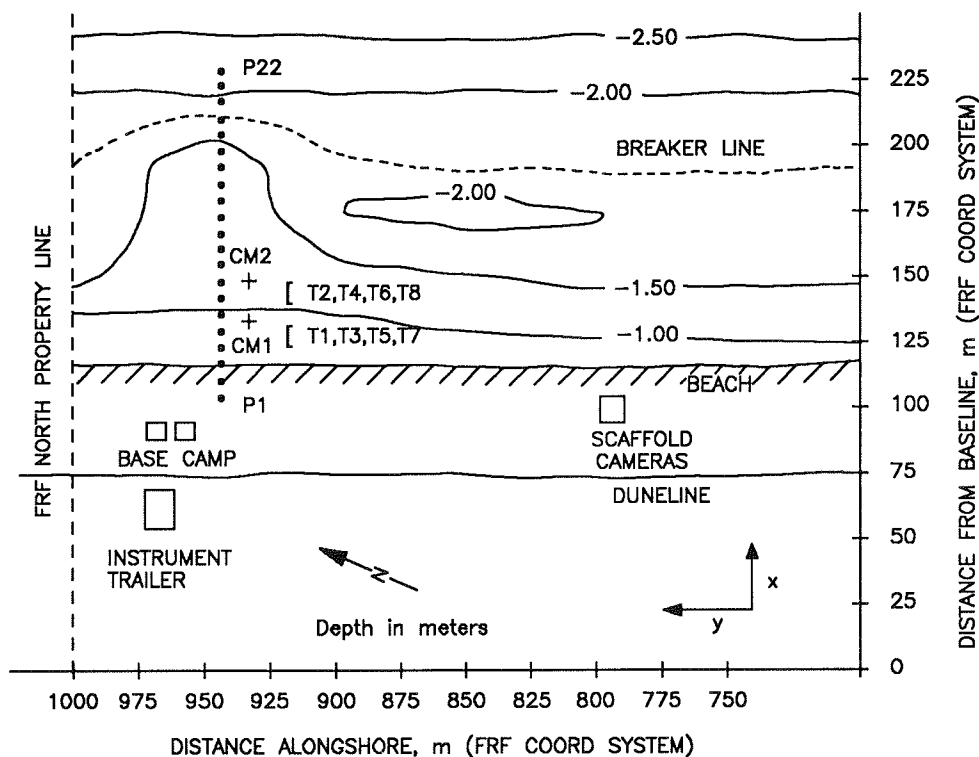
Figure 2. Base camp and typical data collection arrangement

13. The surf zone data collection group consisted of approximately 15 members, and work was divided into four functional areas: sand trapping, measuring currents, measuring waves, and beach profile surveying. These labor-intensive experiments were performed under a range of wind sea and swell conditions with moderate wave heights. Figure 3 shows the energy-based significant wave height H_{mo}* and spectral peak period T_p for 11 to 23 September measured at FRF pressure gage 191. Gage 191 is located at FRF longshore coordinate 990.4 m and cross-shore coordinate 914.4 m, at a depth of -7.77 m relative to National Geodetic Vertical Datum (NGVD), which at the FRF is related to the mean sea level (MSL) datum by MSL(m) = NGVD(m) + 0.067. Tide elevation as recorded on a gage located at the end of the pier is also shown in Figure 3. During the 13 days of intensive data collection (11 to 23 September), H_{mo} ranged from approximately 0.03 to 1.6 m, and T_p ranged from approximately 3 to 14 sec. During most of the project, waves were observed to arrive from slightly out of the southern quadrant, producing a longshore current moving to the north with a magnitude in the range of 0.1 to 0.7 m/sec. Table 1 summarizes the wind and offshore wave regime during the sand-trapping data collection period.

14. A small rip current is frequently located just north of the FRF property line. The data collection arrangement was designed to use the southern longshore feeder current of the rip as a dependable source of a steady and unidirectional longshore current when the direction of the current generated by oblique wave incidence became confused. The longshore sand transport rates and the current moving the sand were produced by combined oblique wave incidence and the rip feeder current. In comparisons made to theoretical expressions, it would be invalid to use predictive formulas for either the longshore current or the longshore sand transport rate that are solely functions of parameters related to obliquely incident waves.

---

* For convenience, symbols and abbreviations are listed in the Notation (Appendix B).

11

Hmo(m)

Tp(sec)

1.6

1.4

1.2

1

0.8

0.6

0.4

0.2

0

14

12

1C

8

6

4

2

0

◇ wave height   + period

11 12 13 14 15 16 17 18 19 20 21 22 23

September 1986

a.   Wave height H_{mo} and period T_p

TIDE ELEVATION, (M)

1.0

0.6

0.2

-0.2

-0.6

-1.0

11   12   13   14   15   16   17   18   19   20   21   22   23   24

SEPTEMBER 1986
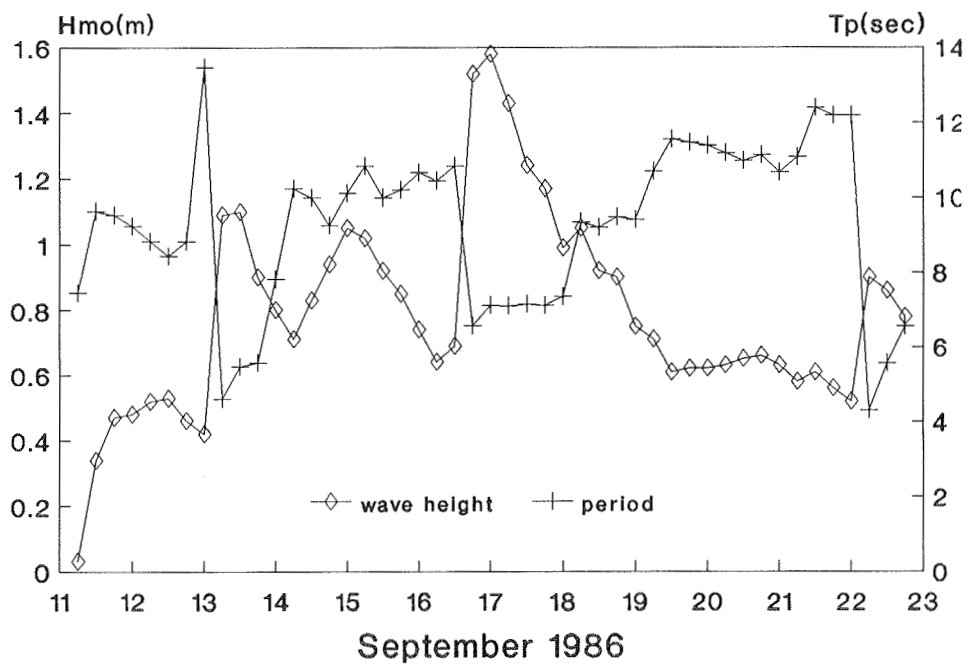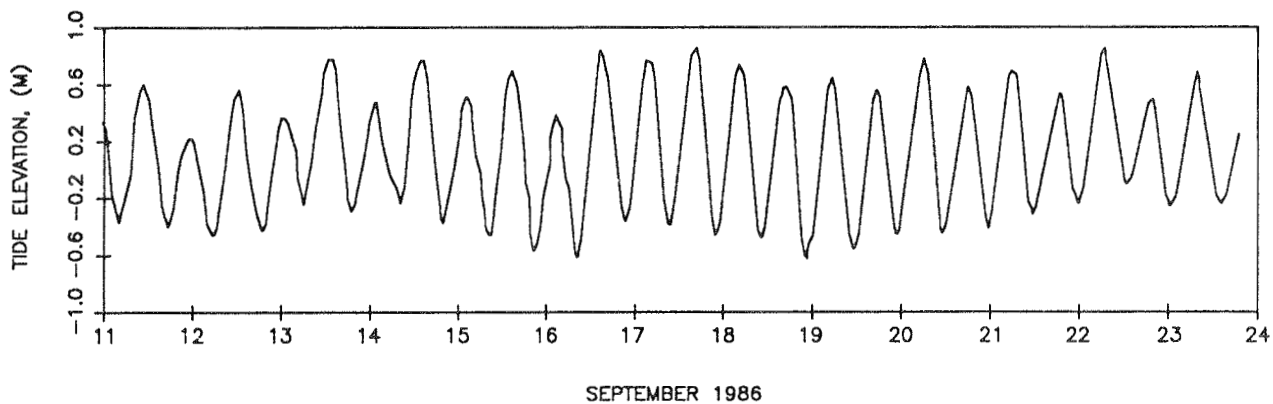
b.   Water level

Figure 3.   Wave height H_{mo} and period T_p measured at FRF gage 191,
and water level recorded at the seaward end of the pier (NGVD datum)

12

Table 1

Summary of Wind and Wave Conditions

Time EDST*	Waves at Gage 191		Wind	
	H_{mo} m	T_p sec	Speed m/sec	Direction deg, TN**
	11 September			
0600	0.03	7.47	2.22	203
1200	0.34	9.63	4.68	183
1800	0.47	9.54	5.50	187
	12 September			
0000	0.48	9.24	6.55	211
0600	0.52	8.84	6.60	220
1200	0.53	8.44	7.39	230
1800	0.46	8.83	3.19	198
	13 September			
0000	0.42	13.47	4.51	310
0600	1.09	4.62	11.28	25
1200	1.10	5.49	8.83	11
1800	0.90	5.58	7.38	13
	14 September			
0000	0.80	7.83	5.51	15
0600	0.71	10.24	3.64	335
1200	0.83	9.99	6.91	24
1800	0.94	9.26	5.56	70
	15 September			
0000	1.05	10.12	3.94	111
0600	1.02	10.84	2.83	120
1200	0.92	9.99	6.14	134
1800	0.85	10.20	3.71	167
	16 September			
0000	0.74	10.67	5.86	210
0600	0.64	10.44	6.05	243
1200	0.69	10.84	12.00	8
1800	1.52	6.58	8.73	41
	17 September			
0000	1.58	7.13	9.63	38
0600	1.43	7.11	8.86	16

(Continued)

* EDST = Eastern Daylight Savings Time.
** TN = True North (shoreline orientation N20°W).

13

Table 1 (Concluded)

Time EDST[*]	Waves at Gage 191		Wind	
	H_{mo} m	T_p sec	Speed m/sec	Direction deg, TN[**]
1200	1.24	7.16	8.61	14
1800	1.17	7.12	6.91	58
	18 September			
0000	0.99	7.36	2.44	81
0600	1.05	9.34	4.23	64
1200	0.92	9.21	3.60	97
1800	0.90	9.48	5.41	142
	19 September			
0000	0.75	9.41	4.07	201
0600	0.71	10.70	3.55	219
1200	0.61	11.56	5.23	244
1800	0.62	11.47	2.33	205
	20 September			
0000	0.62	11.38	1.89	250
0600	0.63	11.18	1.90	258
1200	0.65	10.98	5.14	94
1800	0.66	11.13	3.64	120
	21 September			
0000	0.63	10.67	3.51	113
0600	0.58	11.08	2.99	124
1200	0.61	12.39	2.79	115
1800	0.56	12.19	2.51	78
	22 September			
0000	0.52	12.19	5.57	51
0600	0.90	4.31	7.48	51
1200	0.86	5.57	4.84	55
1800	0.78	6.57	3.80	89

Experiment Arrangement and Measurement Techniques

Surf zone waves and water level

15. The wave height distribution across the surf zone was measured by filming the water surface elevation at 22 target poles made of steel pipe (numbered P1 to P22 in Figure 2) jetted into the sea bottom on a line crossing the surf zone. The poles were spaced at nominal 6-m intervals and painted

14

black to contrast with the white foam on the water surface when reading the films. These poles, called "photopoles," each had two short rods placed horizontally near their top ends and were separated by a known distance (typically, 1 m) to calibrate the wave height measurement. Figure 4 shows the photopole line during SUPERDUCK. Pairs of photopoles were filmed with six synchronized 16-mm professional-grade movie cameras mounted on a 4.5-m-high scaffold located on the beach about 125 m south of the photopole line. The cameras were run in the pulse mode at 5 Hz for a nominal duration of 12.5 min which included a sand trap run. Ebersole and Hughes (in preparation) describe the SUPERDUCK photopole experiments and results.

16. The bottom profile along the photopole line was surveyed each day by means of an infrared beam total survey station housed at the main building of the FRF. These surveys were supplemented by standard transit surveys performed from the base camp and by wide-area surveys taken by the CERC Coastal Research Amphibious Buggy (CRAB). Ebersole and Hughes (in preparation) and FRF (1986) present wide-area bathymetry data. Initially, the nearshore bathymetry in the vicinity of the base camp consisted of an alongshore trough

Figure 4. Photopole line spanning the surf zone

15

and bar form, with a shallower area existing south of the photopole line and a deeper region just north of the photopoles. Spilling breakers mainly predominated in the south region, while plunging breakers occurred to the north. The bathymetry became smoother during the course of the data collection period, making the breaking wave conditions more uniform from north to south. The surf zone bottom consisted of a fine-grained sand substrate with a median grain size of 0.17 mm.

17. The mean water level referenced to NGVD was obtained at 6-min intervals from a tide gage located at the seaward end of the FRF pier (Appendix A, Table A3). The maximum tidal variation observed during the project was approximately 1.4 m (Figure 3). Local mean water levels across the surf zone are tabulated in Ebersole and Hughes (in preparation) for individual data collection runs.

Surf zone currents

18. Water flow was measured with two 2-component Model 551 Marsh-McBirney electromagnetic current meters. The meters were mounted on tripods and connected to shore by cable to recorders located in the instrument trailer. The tripods (Figure 5) were made of 1.9-cm stainless steel rods and stood approximately 1.5 m high. The lower ends of the tripod legs were sunk into the bed to a depth of about 10 cm by shaking the tripod back and forth and applying downward pressure. A tripod with current meter attached was easily moved by two individuals, permitting its rapid relocation in the surf zone in response to varying tide level, wave conditions, and current characteristics. An adjustable collar on the tripod held the metal cylinder housing the meter electronics and preamplifier, allowing vertical adjustment of the current meter sensor. The flow meter sensor was placed 20 to 30 cm above the bed in all deployments. The horizontal axis of the current meter was aligned with its y-component parallel to the trend of the shoreline. The current meters sampled at 5 Hz and recorded for a 10- to 84-min period, depending on the length of the sand-trapping run.

Data collection procedure

19. Longshore sand transport rates were measured by means of portable traps such as shown in Figure 6. A schematic of the trap is given in Figure 7 with only two streamers shown for clarity. The sand collection element of the trap consisted of a metal frame or nozzle to which a cylindrical bag of

16
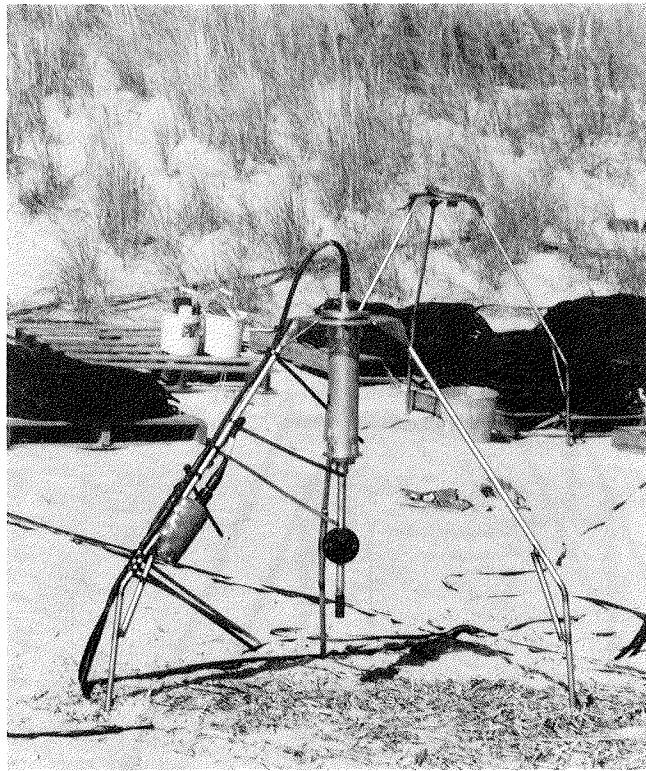
Figure 5.   Current meter mount with
meter installed
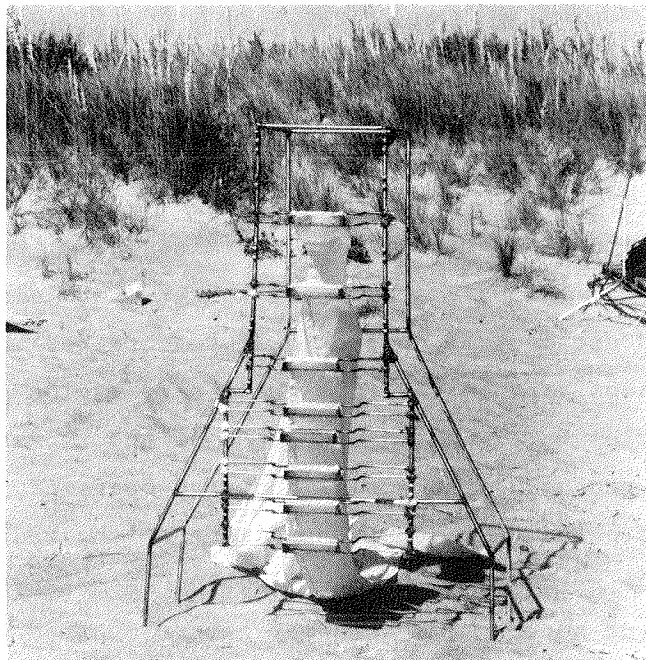
Figure 6.   Streamer traps used at SUPERDUCK
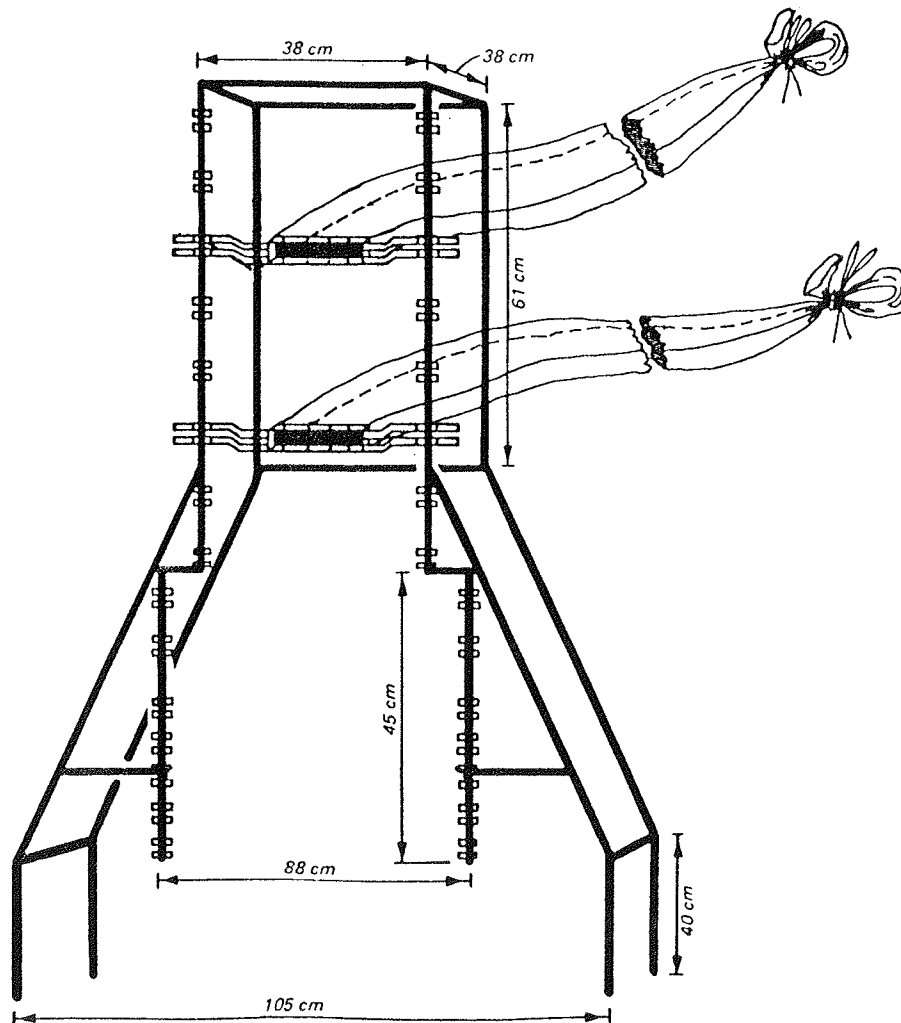
Figure 7. Schematic of the streamer trap rack

flexible filter cloth called a "streamer" was attached. Typically, seven to
nine streamers were mounted vertically on stainless steel racks and pointed in
the direction of flow. The polyester monofilament cloth allowed water to pass
through but retained sediment of nominal diameter greater than the 0.105-mm
mesh, which encompasses sand in the fine grain size region and greater.
Orifices of the nozzles were located upcurrent of the racks and any sediment
clouds due to scour produced by the rack and trap operator. Observation
during operation indicated that scoured sediment at the rack did not move
upstream and into the streamers. Data collection was always performed in a
unidirectional current so that the streamer never reversed direction, a
situation which might cause collected sand to be lost. The concept of the
streamer-type trapping device for use in the nearshore was introduced by

18

Katori (1982, 1983). Development of the trap has continued at CERC, including mounting of the streamers on various types of racks (Kraus 1987) and optimization of the trap nozzle geometry (Rosati and Kraus 1988, 1989). Although the wide-base SUPERDUCK racks shown in Figures 6 and 7 were stable under relatively high waves, trap operators preferred the less awkward rectangular racks used at DUCK85 (see Kraus, Gingerich, and Rosati 1989).

20. The nozzles on the traps used at SUPERDUCK had a width of 15 cm and a height of 2.5 cm, with a 9.5-mm-thick stainless steel "hood" 5.1 cm in length (Figure 8). Nozzles were attached to the trap racks by 6.4-mm stainless steel mounting bars welded to the nozzles that were positioned in circular fasteners on the trap frame and secured in place with duct tape (Figure 7).

21. During the DUCK85 data collection project (Kraus, Gingerich, and Rosati 1989), highly favorable sea conditions characterized by "clean" swell with moderate wave heights facilitated extensive measurements of the variation of the longshore sand transport rate through the surf zone. Traps were positioned from near the shoreline to the breaker line, with two current meters located at representative locations in the surf zone, and sand transport was measured for 5- and 10-min periods. These measurements resulted in a high-quality data set on the cross-shore distribution of the longshore sand transport rate, which could be integrated to obtain the total transport rate as a function of representative wave and current conditions. This method of measuring sand transport, in which traps are positioned across the surf zone, is referred to as the Spatial Sampling Method (SSM).
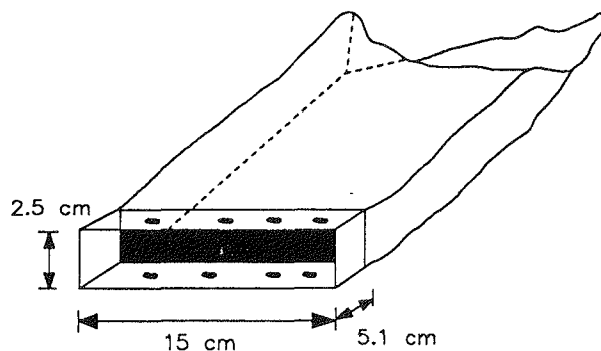
Figure 8. SUPERDUCK streamer nozzle

22. Recognizing a need for more accurate prediction of sand transport at a point as a function of waves and currents at that position, a Temporal Sampling Method (TSM) was used during the SUPERDUCK experiment. In the TSM, one or two traps were repeatedly deployed at one or two points in the surf zone, with corresponding wave and current measurements made in the same region. If two traps were deployed in close proximity (about 1 m apart), an indication of reliability between two traps under similar hydrodynamic conditions was obtained, termed a "consistency test." The TSM runs resulted in high-quality measurements of the sand transport rate as a function of local waves and currents through time, at 5-min intervals for as long as an 84-min data collection period.

23. To measure the transport rate during a typical TSM run, two traps (denoted by symbols T1 and T2 in Figure 2) were carried to predetermined positions located updrift of current meters (denoted by symbols CM1 and CM2 in Figure 2), and referenced to the photopole line. Usually one person carried and operated one trap; however, two operators were necessary if surf zone conditions were rough or if the traps were positioned at the breaker line. At a signal, the racks were simultaneously thrust into the bed with the nozzles oriented into the longshore current. Horizontal bars along the bottom of two sides of the rack could be stepped on to bury the 40-cm-long legs. At complete burial of the rack legs, the horizontal bars prevented further penetration of the legs and kept the lowermost streamer nozzle at the bed. During the course of a trap deployment (typically of 5- to 10-min duration), the trap operator would periodically step on the horizontal bars to keep the trap legs fully buried and to counter wave and current action, which would tend to tilt the trap shoreward and downstream, respectively. In weak long-shore currents, the streamers would wrap around the vertical bars of the rack with passage of waves, requiring the trap operator to untangle them. In moderate to strong currents (greater than approximately 20 cm/sec), the streamers would fully extend in the flow and require little attention from the trap operator. Figure 9 shows the traps being deployed in a TSM run.

24. At the end of the first sampling period, a signal was given from the beach, and the two traps were pulled from the bed as the second set (denoted by the symbols T3 and T4 in Figure 2) was deployed at approximately the same locations in the surf zone. The first two traps were lifted above

20

Figure 9. Streamer traps deployed in a TSM run

the water and brought to shore (Figure 10), and collected sand was washed from the streamers with seawater into small patches of filter cloth. The sand sample and cloth (of known weight when wet) were weighed in the drip-free condition (Kraus and Nakashima 1986). Samples from all traps from one run per day were retained for drying and grain size analysis in the laboratory. The dry weights obtained allowed calibration of the drip-free to dry weight conversion factor. Deployment of trap pairs continued (denoted by the symbols T5 through T8 in Figure 2) for data collection periods from 23 to 84 min in length.

25. Between experiment runs, the trapped sand weights were plotted to understand qualitative aspects of the transport conditions and to design the next series of runs, such as positioning of traps and length of temporal sampling. For example, from inspection of the transport rate distribution through the water column, a supporting cross-bar on the trap frame was found to partially block sand transport into the second streamer above the bed. During succeeding data collection, the second streamer was positioned away from the cross-bar, eliminating the problem. The capability to analyze the

21

Figure 10. Traps being removed from the surf zone

transport rate data onsite is considered one of the important advantages of using traps, enabling a quality control check on trap operation and early interpretation of results for adjustment of experimental design.

Transport Rate Analysis

26. Procedures for calculating transport rates from the raw data are described in this section. The streamers measure a sand flux, i.e., the weight of sand passing through the nozzle of a certain cross-sectional area during the sampling interval. If sampling is performed in a unidirectional flow, as was the case in these experiments, no sand coarser than 0.105 mm is lost once it has entered the streamer, and the flux can be directly associated with the current to develop predictive empirical relations. The raw data of sand weight collected in the streamers are listed in Table A1 of Appendix A.

27. The flux of sand F at streamer k is given by

$$F(k) = \frac{S(k)}{\Delta h \Delta w \Delta t} \tag{1}$$

in which

   F = sand flux, kg/(m²-sec)

   k = streamer number, increasing in order from the bottom (k = 1)
       to the last streamer (k = N)

   S = dry weight of sand, kg (force)

   Δh = height of streamer nozzle (0.025 m for SUPERDUCK)

   Δw = width of streamer nozzle (0.15 m for SUPERDUCK)

   Δt = sampling time interval, sec

The flux between adjacent streamers $FE(k)$ can be estimated by linear
interpolation using adjacent measured values

$$FE(k) = 0.5[F(k) + F(k+1)] \tag{2}$$

28. The total transport rate per unit width i at a particular trap is
calculated by using the determined fluxes and distances $\Delta a(k)$ between
nozzles,

$$i = \Delta h \sum_{k=1}^{N} F(k) + \sum_{k=1}^{N} \Delta a(k) FE(k) \tag{3}$$

in which N is the total number of streamers on the trap. The first summa-
tion term represents the actual measured fluxes, and the second summation term
represents the interpolated fluxes between nozzles. If traps were placed on a
line across the surf zone (SSM), transport rates per unit width were calcu-
lated with Equation 3, and the trapezoid rule was used to compute the total
longshore sand transport rate across the surf zone. Elevations of the
streamers above the bed are listed in Table A2 of Appendix A.

29. Sand-trapping efficiency tests in uniform flow were performed in a
series of experiments (Rosati and Kraus 1989) for nozzle configurations which
had near-optimal hydraulic efficiencies (Rosati and Kraus 1988), including the
DUCK85 and SUPERDUCK nozzles. It was found that the SUPERDUCK nozzle had a

23

sand-trapping efficiency near unity (1.02 ± 0.03) for suspended sand, but a lower efficiency for a nozzle resting on the bed (0.68 ±.0.31). Sand fluxes presented herein have been corrected for bottom nozzle efficiency by dividing the quantity of sand obtained by the bed-load trapping efficiency. Sand fluxes were not modified for the suspended nozzles, as the efficiency value for these nozzles is nearly unity.

30. The lower value (0.68 ± 0.31) of the bed-load trapping efficiency (which includes suspended load within 2.5 cm of the bottom) is caused by scour and the scour hole created under the nozzle that was occasionally observed to occur during portions of the testing period. The actual efficiency of the streamer trap in intersecting oscillatory and quasi-steady uniform flow in the surf zone is not known, but qualitative evaluation using field observations indicates that efficiencies in the surf zone are similar to those determined in the uniform flow tank under sheet flow conditions.

PART III: RESULTS

31.   This chapter lists and explains the principal data on transport
rates, currents, and waves obtained in the September phase surf zone experi-
ments at SUPERDUCK.   Selected results are also presented to introduce the
characteristics and potential uses of the data set.

Orientation to the Measurement Runs

32.   Four types of sand transport rate data collection runs were per-
formed using the traps:

a.   Measurement of the temporal distribution of the longshore
     sand transport rate at one or two points in the surf zone (TSM
     run).

b.   Measurement of the cross-shore distribution of the longshore
     sand transport rate (SSM run).

c.   Measurement of transport rates at neighboring locations
     (typically 1 m apart) (consistency test).

d.   Measurement of the transport rate in a rip current.

Seven to nine streamers mounted on the racks provided the vertical distribu-
tion of the sand flux.

33.   Data collection runs documented in this report are listed in
Table 2.   Each run is assigned a number, as shown in the first column, which
uniquely identifies it by the date and time the sampling was conducted.   The
concatenation of numbers comprising a run identification (ID) gives the year
(86), month (9), day (11 to 23), and start time of the run in EDST as hours
and minutes on a 24-hr clock.   Current velocity and wave measurement (photo-
pole) ID numbers are similarly defined.   Current meters and movie cameras were
often started a minute or two before the corresponding sand trap run began.
Trap and current meter deployment intervals and locations in the surf zone
relative to the photopole line are given in Table 3, and locations of the
photopoles in the FRF coordinate system are presented in Table A4.

Table 2

Summary of Surf Zone Sand Trap Data and Tide Condition

Run ID No.	Time, EDST	Data Collection	No. Traps	Tide
8609111745*	1745-1755	SSM	6	Falling
8609121037	1037-1047	Rip Current	6	Low
8609151345*	1345-1408	TSM	3 pairs	Rising
8609151630*	1630-1654	TSM	3	Rising
8609160922	0922-0932	Consistency	1 pair	Falling
8609160945*	0945-0955	Consistency	1 pair	Falling
8609161116*	1116-1126	SSM	10	Falling
8609181225*	1225-1249	TSM	4 pairs	Falling
8609181453*	1453-1524	TSM	5 pairs	Falling
8609191016*	1016-1026	SSM	6	High
8609191230	1230-1254	TSM	4 pairs	Falling
8609201045*	1045-1133	TSM	8	High
8609201500*	1500-1548	TSM (incl 2 consistency)	10	Low
8609211046	1046-1056	Consistency	1 pair	High
8609211345	1345-1509	TSM (incl 2 consistency)	16	Falling
8609220730	0730-0810	TSM	8	Rising
8609221600	1600-1625	TSM	5 pairs	Rising
8609221750	1750-1756	SSM	10	Low
8609231035	1035-1100	TSM	5	Rising

* Complete or partial wave data set presently available (presented herein or by Ebersole and Hughes (in preparation)).

Table 3

Times and Locations of Trap and Current Meter Deployments

Run ID No.	Trap/Current Meter Number	Time EDST	Approximate Location Relative to Photopoles
8609111745	T1	1745-1755	P4-P5*, north of photopoles
	T2		P7-P8, north of photopoles
	T3		P8-P9, north of photopoles
	T4		P9-P10, north of photopoles
	T5		P11-P12, north of photopoles
	T6		P13-P14, north of photopoles
8609121037	T1	1037-1047	45 m offshore, rip throat
	T2		30 m offshore, rip throat
	T3		23 m offshore, rip throat
	T4		5 m offshore, north feeder
	T5		15 m offshore, rip throat
	T6		9 m offshore, south feeder
8609151345	T1	1345-1352	P6-P7, south of photopoles
	T2	1345-1352	P6-P7, north of photopoles
	T3	1352-1400	P6-P7, south of photopoles
	T4	1352-1400	P6-P7, north of photopoles
	T5	1400-1408	P6-P7, south of photopoles
	T6	1400-1408	P6-P7, north of photopoles
	CM1	1345-1408	P6-P7, south of photopoles
	CM2	1345-1408	P6-P7, north of photopoles
8609151630	T3	1630-1638	P3-P4, south of photopoles
	T5	1638-1646	P3-P4, south of photopoles
	T7	1646-1654	P3-P4, south of photopoles
	CM1	1630-1654	P4, south of photopoles
	CM2	1630-1654	P4, north of photopoles
8609160922	T1	0922-0932	P7-P8, south of photopoles
	T2	0922-0932	P7-P8, south of photopoles
	CM1	0922-0932	P7, south of photopoles
8609160945	T8	0945-0955	P8-P9, south of photopoles
	T9	0945-0955	P8-P9, south of photopoles
	CM1	0945-0955	P8, south of photopoles

(Continued)

* The notation P4-P5 indicates that trap was located midway between photo-poles P4 and P5.

(Sheet 1 of 5)

27

Table 3 (Continued)

Run ID No.	Trap/Current Meter Number	Time EDST	Approximate Location Relative to Photopoles
8609161116	T1	1116-1126	P6-P7, north of photopoles
	T2		P7-P8, north of photopoles
	T3		P8-P9, north of photopoles
	T4		P9-P10, north of photopoles
	T5		P10-P11, north of photopoles
	T6		P11-P12, north of photopoles
	T7		P12-P13, north of photopoles
	T8		P13-P14, north of photopoles
	T9		P14-P15, north of photopoles
	T10		P15-P16, north of photopoles
	CM1		P9, south of photopoles
	CM2	↓	P12, south of photopoles
8609181225	T1	1225-1231	P6, south of photopoles
	T2	1225-1231	P8, south of photopoles
	T3	1231-1237	P6, south of photopoles
	T4	1231-1237	P8, south of photopoles
	T5	1237-1243	P6, south of photopoles
	T6	1237-1243	P8, south of photopoles
	T7	1243-1249	P6, south of photopoles
	T8	1243-1249	P8, south of photopoles
	CM1	1225-1249	P6, south of photopoles
	CM2	1225-1249	P8, south of photopoles
8609181453	T1	1453-1459	P7, south of photopoles
	T2	1453-1459	P9, south of photopoles
	T3	1459-1505	P7, south of photopoles
	T4	1459-1505	P9, south of photopoles
	T5	1505-1511	P7, south of photopoles
	T6	1505-1511	P9, south of photopoles
	T7	1511-1518	P7, south of photopoles
	T8	1511-1518	P9, south of photopoles
	T9	1518-1524	P7, south of photopoles
	T10	1518-1524	P9, south of photopoles
	CM1	1453-1524	P7, south of photopoles
	CM2	1453-1524	P9, south of photopoles
8609191016	T3	1016-1026	P4-P5, south of photopoles
	T4		P1-P2, south of photopoles
	T5		P2-P3, south of photopoles
	T6	↓	P3-P4, south of photopoles

(Continued)

Table 3 (Continued)

Run ID No.	Trap/Current Meter Number	Time EDST	Approximate Location Relative to Photopoles
8609191016	T9	1016-1026	P5-P6, south of photopoles
	T10		P6-P7, south of photopoles
	CM1		P5, south of photopoles
	CM2		P7, south of photopoles
8609191230	T1	1230-1236	P6, south of photopoles
	T2	1230-1236	P7-P8, south of photopoles
	T3	1236-1242	P6, south of photopoles
	T4	1236-1242	P7-P8, south of photopoles
	T5	1242-1248	P6, south of photopoles
	T6	1242-1248	P7-P8, south of photopoles
	T7	1248-1254	P6, south of photopoles
	T8	1248-1254	P7-P8, south of photopoles
	CM1	1243-1254	P6, south of photopoles
	CM2	1243-1254	P7-P8, south of photopoles
8609201045	T1	1045-1051	P5-P6, south of photopoles
	T2	1051-1057	
	T3	1057-1103	
	T4	1103-1109	
	T5	1109-1115	
	T6	1115-1121	
	T7	1121-1127	
	T8	1127-1133	
	CM1	1045-1133	
	CM2	1045-1133	
8609201500	T1	1500-1506	P8-P9, south of photopoles
	T2	1506-1512	
	T3	1512-1518	
	T4	1518-1524	
	T5	1524-1530	
	T6	1530-1536	
	T7	1536-1542	
	T8	1536-1542	
	T9	1542-1548	
	T10	1542-1548	
	CM1	1500-1548	P8, south of photopoles
	CM2	1500-1548	P9, south of photopoles

(Continued)

Table 3 (Continued)

Run ID No.	Trap/Current Meter Number	Time EDST	Approximate Location Relative to Photopoles
8609211046	T1	1046-1056	P6, south of photopoles
	T2		P6, south of photopoles
	CM1		P5-P6, south of photopoles
	CM2		P5-P6, south of photopoles
8609211345	T1	1345-1351	P8-P9, south of photopoles
	T2	1351-1357	
	T3	1357-1403	
	T4	1403-1409	
	T5	1403-1409	
	T6	1409-1415	
	T7	1415-1421	
	T8	1415-1421	
	T9	1421-1427	
	T10	1427-1433	
	T11	1433-1439	
	T12	1439-1445	
	T13	1445-1451	
	T14	1451-1457	
	T15	1457-1503	
	T16	1503-1509	
	CM1	1345-1509	P8, south of photopoles
	CM2	1345-1509	P9, south of photopoles
8609220730	T1	0730-0735	P7, south of photopoles
	T2	0735-0740	P9, south of photopoles
	T3	0740-0745	P7, south of photopoles
	T4	0745-0750	P9, south of photopoles
	T5	0750-0755	P7, south of photopoles
	T6	0755-0800	P9, south of photopoles
	T7	0800-0805	P7, south of photopoles
	T8	0805-0810	P9, south of photopoles
	CM1	0730-0810	P7, south of photopoles
	CM2	0730-0810	P9, south of photopoles
8609221600	T1	1600-1605	P5-P6, south of photopoles
	T2	1600-1605	
	T3	1605-1610	
	T4	1605-1610	
	T5	1610-1615	
	T6	1610-1615	
	T7	1615-1620	

(Continued)

Table 3 (Concluded)

Run ID No.	Trap/Current Meter Number	Time EDST	Approximate Location Relative to Photopoles
8609221600	T8	1615-1620	P5-P6, south of photopoles
	T9	1620-1625	P5-P6, south of photopoles
	T10	1620-1625	P5-P6, south of photopoles
	CM1	1600-1625	P5, south of photopoles
	CM2	1600-1625	P6, south of photopoles
8609221750	T1	1750-1756	P5, south of photopoles
	T2		P6, south of photopoles
	T3		P7, south of photopoles
	T4		P8, south of photopoles
	T5		P9, south of photopoles
	T6		P10, south of photopoles
	T7		P11, south of photopoles
	T8		P12, south of photopoles
	T9		P13, south of photopoles
	T10		P14, south of photopoles
	CM1		P7, south of photopoles
	CM2		P9, south of photopoles
8609231035	T1	1035-1040	P4-P5, south of photopoles
	T2	1040-1045	
	T3	1045-1050	
	T4	1050-1055	
	T5	1055-1100	
	CM1	1035-1100	P4, south of photopoles
	CM2	1035-1100	P5, south of photopoles

(Sheet 5 of 5)

Temporal Sampling Method (TSM)

34. Emphasis was placed on measurement of the temporal distribution of the longshore transport rate at one or two points in the surf zone during SUPERDUCK. In measuring the temporal behavior of the transport rate, the vertical distribution of the sand flux was obtained at each trap. Eleven TSM runs were conducted. Complete wave and current data are presently available for six runs conducted on 15, 18, and 20 September.

Cross-shore measurement (SSM)

35. Four runs were conducted to measure the cross-shore distribution of the longshore sand transport rate, three with a northerly directed longshore

31

current and one with a southerly directed current. Complete photopole and current data sets are available for two runs (only photopole data are available for Run 8609111745).

Consistency tests

36. Consistency tests were performed to compare collected quantities of sand from traps placed in close proximity to each other. These tests were used as an indicator of trap reproducibility and reliability in the field. In the consistency tests, two traps were placed in the surf zone approximately 1 m apart. The seaward trap was located a distance sufficiently downdrift of the shoreward trap (typically, about 1 m) so that sand scoured from the seaward trap and transported shoreward with the incoming waves would not be collected by the shoreward trap. Consistency testing was conducted as a part of several TSM runs by deploying trap pairs. Waves and currents were measured during consistency tests, and all current meter data have been analyzed; however, wave data sets are only available for TSM Run 8609201500 (includes two consistency tests) and Consistency Run 8609160945 (partial wave data set) (see Ebersole and Hughes, in preparation).

Rip current measurement

37. An experiment was performed on 12 September with the objective of measuring sand transport in the rip current located near the north FRF property line. Two traps were placed in the south longshore feeder current of the rip, one trap in the north feeder current, and three traps in the throat of the rip. Streamers on traps placed in the strong offshore current flow in the rip throat extended seaward, directly against the incident waves. Neither current nor wave data are available for the rip current run.

Currents

38. The two current meters bracketed the deployed traps, and were placed slightly down-current. The meters were moved as necessary as trap deployment location changed with the tide. The basic processed current speed data (mean and standard deviation) are given in Table 4 for 17 runs. Columns in Table 4 represent x- and y-components of the current in the experiment coordinate system, for the meters 1 and 2. The x-axis points offshore

Table 4

Surf Zone Current Measurements

Time EDST	CY1 Mean	σ_v	CX1 Mean	σ_v	CY2 Mean	σ_v	CX2 Mean	σ_v
				Current Speed, m/sec				
				Run 8609151345				
1345-1352	0.283	0.239	-0.019	0.429	0.244	0.186	-0.015	0.413
1353-1400	0.275	0.203	-0.033	0.506	0.207	0.211	-0.017	0.445
1401-1408	0.343	0.233	-0.061	0.468	0.241	0.189	-0.036	0.406
				Run 8609151630				
1630-1638	0.540	0.336	-0.242	0.707	0.564	0.234	-0.162	0.668
1639-1646	0.577	0.370	-0.259	0.764	0.523	0.237	-0.173	0.659
1647-1654	0.620	0.325	-0.273	0.767	0.576	0.240	-0.141	0.629
				Run 8609160922				
0922-0932	0.303	0.195	-0.047	0.351	--	--	--	--
				Run 8609160945				
0945-0955	0.289	0.187	0.071	0.379	--	--	--	--
				Run 8609161116				
1116-1126	0.178	0.194	0.073	0.373	0.227	0.193	0.075	0.345
				Run 8609181225				
1225-1231	0.338	0.244	-0.211	0.510	0.357	0.186	-0.077	0.388
1232-1237	0.382	0.244	-0.203	0.561	0.356	0.206	-0.061	0.407
1238-1243	0.421	0.213	-0.192	0.588	0.483	0.166	-0.035	0.459
1244-1249	0.400	0.233	-0.180	0.537	0.492	0.181	0.003	0.405
				Run 8609181453				
1453-1459	0.344	0.154	-0.073	0.417	0.394	0.161	0.060	0.368
1500-1505	0.349	0.168	-0.051	0.449	0.344	0.169	0.025	0.408
1506-1511	0.423	0.184	-0.109	0.506	0.475	0.185	0.016	0.406
1512-1518	0.404	0.159	-0.088	0.434	0.336	0.170	0.051	0.382
1519-1524	0.393	0.162	-0.089	0.430	0.402	0.176	0.017	0.364
				Run 8609191016				
1016-1026	0.154	0.166	-0.073	0.512	0.186	0.158	-0.045	0.444
				Run 8609191230				
1230-1236	--	--	--	--	--	--	--	--
1237-1242	--	--	--	--	--	--	--	--

(Continued)

(Sheet 1 of 3)

Table 4 (Continued)

Time EDST	Current Speed, m/sec							
	CY1		CX1		CY2		CX2	
	Mean	σ_v	Mean	σ_v	Mean	σ_v	Mean	σ_v
1243-1248	0.411	0.203	-0.146	0.213	0.421	0.203	0.013	0.420
1249-1254	0.364	0.165	-0.085	0.461	0.336	0.160	0.040	0.423
Run 8609201045								
1045-1051	0.154	0.193	-0.114	0.562	0.130	0.122	-0.105	0.477
1052-1057	0.224	0.173	-0.115	0.556	0.225	0.136	-0.088	0.472
1058-1103	0.209	0.191	-0.115	0.520	0.247	0.132	-0.075	0.422
1104-1109	0.207	0.242	-0.041	0.472	0.206	0.136	-0.043	0.419
1110-1115	0.091	0.185	-0.146	0.563	0.074	0.139	-0.084	0.451
1116-1121	0.190	0.179	-0.216	0.549	0.192	0.123	-0.083	0.480
1122-1127	0.195	0.203	-0.154	0.508	0.160	0.136	-0.057	0.410
1128-1133	0.247	0.186	-0.184	0.519	0.236	0.161	-0.068	0.409
Run 8609201500								
1500-1506	0.596	0.159	0.018	0.389	0.603	0.175	-0.070	0.394
1507-1512	0.559	0.157	0.044	0.356	0.559	0.172	-0.035	0.363
1513-1518	0.472	0.128	0.017	0.350	0.511	0.161	-0.058	0.371
1519-1524	0.550	0.152	0.036	0.337	0.554	0.172	-0.054	0.371
1525-1530	0.449	0.156	0.032	0.362	0.482	0.142	-0.029	0.383
1531-1536	0.564	0.159	0.022	0.367	0.587	0.153	-0.056	0.387
1537-1542	0.357	0.024	0.032	0.379	0.392	0.135	0.001	0.369
1543-1548	0.319	0.022	0.011	0.388	0.344	0.167	-0.027	0.400
Run 8609211046								
1046-1056	0.149	0.134	-0.093	0.435	0.052	0.103	-0.056	0.417
Run 8609211345								
1345-1351	0.185	0.214	-0.019	0.365	0.138	0.109	-0.054	0.339
1352-1357	0.291	0.147	-0.083	0.435	0.173	0.123	-0.094	0.374
1358-1403	0.266	0.147	-0.049	0.418	0.217	0.126	-0.034	0.360
1404-1409	0.255	0.146	-0.001	0.436	0.199	0.132	-0.033	0.365
1410-1415	0.247	0.169	-0.055	0.434	0.163	0.146	-0.077	0.383
1416-1421	0.351	0.142	-0.044	0.453	0.276	0.124	-0.050	0.386
1422-1427	0.293	0.149	-0.039	0.437	0.163	0.122	-0.037	0.387
1428-1433	0.439	0.161	-0.057	0.422	0.295	0.142	-0.035	0.376
1434-1439	0.391	0.121	-0.017	0.425	0.261	0.109	-0.010	0.349
1440-1445	0.419	0.137	-0.028	0.397	0.250	0.132	-0.020	0.342
1446-1451	0.529	0.139	-0.077	0.431	0.335	0.138	-0.028	0.379
1452-1457	0.460	0.162	-0.009	0.420	0.301	0.124	0.000	0.358

(Continued)

Table 4 (Concluded)

Time EDST	CY1		CX1		CY2		CX2	
	Mean	σ_v	Mean	σ_v	Mean	σ_v	Mean	σ_v
				Current Speed, m/sec				
1458-1503	0.487	0.204	-0.050	0.454	0.345	0.166	-0.017	0.397
1504-1509	0.494	0.161	-0.052	0.422	0.369	0.127	-0.025	0.359
			Run 8609220730					
0730-0735	-0.541	0.268	-0.249	0.443	-0.422	0.232	-0.102	0.464
0736-0740	-0.549	0.295	-0.251	0.426	-0.481	0.215	-0.097	0.464
0741-0745	-0.657	0.290	-0.295	0.433	-0.573	0.214	-0.128	0.472
0746-0750	-0.533	0.287	-0.202	0.453	-0.473	0.223	-0.106	0.459
0751-0755	-0.597	0.290	-0.083	0.486	-0.465	0.245	-0.105	0.479
0756-0800	-0.690	0.263	-0.124	0.224	-0.515	0.212	-0.140	0.469
0801-0805	-0.607	0.262	-0.119	0.469	-0.492	0.209	-0.113	0.466
0806-0810	-0.512	0.264	-0.151	0.457	-0.399	0.252	-0.126	0.456
			Run 8609221600					
1600-1605	-0.522	0.243	-0.187	0.359	-0.537	0.172	-0.031	0.336
1606-1610	-0.489	0.247	-0.148	0.361	-0.508	0.179	0.010	0.350
1611-1615	-0.356	0.247	-0.177	0.385	-0.367	0.185	-0.098	0.369
1616-1620	-0.378	0.253	-0.182	0.382	-0.369	0.171	-0.082	0.366
1621-1625	-0.357	0.231	-0.156	0.369	-0.384	0.159	-0.052	0.345
			Run 8609221750					
1750-1756	-0.372	0.226	-0.154	0.382	-0.396	0.176	0.057	0.341
			Run 8609231035					
1035-1040	0.043	0.201	-0.201	0.544	-0.025	0.166	-0.077	0.494
1041-1045	0.042	0.166	-0.203	0.533	-0.020	0.141	-0.131	0.468
1046-1050	0.004	0.184	-0.189	0.522	0.007	0.140	-0.084	0.508
1051-1055	0.075	0.199	-0.116	0.556	-0.003	0.118	-0.066	0.533
1056-1100	-0.026	0.154	-0.071	0.502	0.015	0.122	-0.037	0.451

(Sheet 3 of 3)

(positive x-component indicates seaward-directed flow), and the y-axis points north. Current meter 1 was located shoreward of current meter 2.

39. The mean current speed and standard deviation were calculated for the indicated trap sampling interval. Most x-components of the mean current are negative, indicating that the flow was primarily directed onshore at an elevation of approximately 20 cm from the bed where the current meter sensors were located. The y-components of the mean current are positive, except for

runs conducted on 22 and 23 September, indicating that the longshore current flowed from south to north (toward the rip current) on the majority of experiment days. The streamers were observed to reverse direction only during one TSM run on 23 September. As expected, the mean longshore current (y-component) is larger than the mean cross-shore current (x-component). The standard deviation of the cross-shore component (σ_v of x-component) is larger than the standard deviation of the longshore component (σ_v of y-component), because of the oscillatory motion of incident waves.

Waves and Water Levels

40. The analysis procedure for obtaining wave and water level parameters from the photopole record is described in detail by Ebersole and Hughes (in preparation). In summary, the digitized time series was cleaned through visual inspection and then filtered to remove long-period wave motions. The filter eliminated oscillations with periods greater than 30 sec and preserved oscillations with periods less than 16 sec; waves with periods between 16 and 30 sec were partially retained (Ebersole and Hughes, in preparation). Table 5 presents various statistical properties of the filtered record corresponding to each trap deployment interval (6, 7, or 8 min) in the six TSM runs for which photopole data were analyzed. Listed wave properties were calculated through an individual wave zero-down crossing method.

Sand Transport

Consistency runs

41. Seven consistency tests were conducted during SUPERDUCK, and vertical distributions of the fluxes measured with the two closely spaced traps, designated by "shoreward" and "seaward" locations, have been plotted to the same scales for comparison (Figures 11 through 17). Four of the consistency comparisons were conducted as a part of TSM runs 8609201500 and 8609211345 (Figure 13, 14, 16, and 17) and are differentiated with the notation "-1" and "-2" at the end of the run number. The shape of the vertical distributions of sand flux measured during SUPERDUCK varied more between the shoreward and seaward traps than those measured during DUCK85 (see

Table 5

Summary of Wave Parameters

Time EDST	Photo-pole	H* m	Var(H) m²	S(H) m	Skew(H)	Kurt(H)	Hmax m	Hmin m	T sec	Var(T) sec²	S(T) sec	Skew(T)	Kurt(T)	Tmax sec	Tmin sec	Hrms m	Hs m	H10 m	Trms sec	Ts sec	T10 sec
									Run 8609151345												
1345-1352	6	0.47	0.016	0.13	0.03	3.66	0.80	0.18	9.32	15.83	3.98	0.83	3.75	21.80	3.60	0.49	0.59	0.73	10.12	13.68	17.93
1352-1400	6	0.49	0.021	0.15	-0.42	3.19	0.82	0.13	9.01	10.17	3.19	0.16	2.27	16.00	3.20	0.51	0.64	0.73	9.55	12.53	14.96
1400-1408	6	0.51	0.011	0.11	-0.68	3.86	0.72	0.19	9.65	9.42	3.07	0.34	2.57	17.00	3.20	0.52	0.61	0.67	10.12	13.21	15.60
1345-1352	7	0.52	0.020	0.14	-0.62	2.82	0.73	0.18	9.25	15.62	3.95	1.49	6.39	22.80	3.20	0.54	0.67	0.71	10.04	13.06	17.75
1352-1400	7	0.56	0.016	0.13	-0.58	3.38	0.84	0.18	9.59	13.61	3.69	1.44	6.61	24.40	3.80	0.57	0.68	0.75	10.26	13.35	18.20
1400-1408	7	0.53	0.013	0.11	-0.56	3.82	0.74	0.20	9.72	13.86	3.72	0.62	2.69	18.40	4.00	0.54	0.65	0.72	10.40	13.96	17.50
1345-1352	8	0.53	0.021	0.15	-0.71	3.43	0.78	0.15	8.91	10.48	3.24	0.10	2.63	16.60	3.40	0.55	0.67	0.75	9.47	12.33	14.75
1352-1400	8	0.54	0.028	0.17	-0.51	3.18	0.87	0.10	8.87	13.18	3.63	0.23	2.19	17.40	3.40	0.57	0.71	0.81	9.57	12.88	15.52
1400-1408	8	0.56	0.019	0.14	-0.56	3.67	0.79	0.18	9.48	8.07	2.84	-0.05	2.46	16.00	3.60	0.58	0.71	0.78	9.89	12.45	13.88
									Run 8609151630												
1630-1638	3	0.61	0.031	0.18	-0.28	2.91	0.99	0.17	8.15	10.52	3.24	0.45	2.41	17.00	3.20	0.63	0.79	0.91	8.76	12.09	13.96
1638-1646	3	0.61	0.027	0.17	0.08	3.98	1.08	0.13	8.48	12.86	3.59	0.83	3.27	19.20	3.60	0.63	0.78	0.93	9.19	12.53	16.20
1646-1654	3	0.51	0.025	0.16	-0.12	2.06	0.79	0.18	7.93	15.47	3.93	1.26	4.63	21.80	3.20	0.53	0.69	0.76	8.84	12.42	17.04
1630-1638	4	0.66	0.023	0.15	-0.41	3.72	0.96	0.18	9.00	6.83	2.61	-0.66	2.64	13.80	3.40	0.68	0.81	0.93	9.36	11.43	12.85
1638-1646	4	0.63	0.040	0.20	-0.30	2.64	1.07	0.15	7.28	7.97	2.82	0.33	2.07	13.60	3.20	0.66	0.85	0.94	7.80	10.61	12.47
1646-1654	4	0.72	0.036	0.19	-0.92	3.21	1.01	0.23	8.17	9.04	3.01	0.36	2.61	17.00	3.20	0.74	0.90	0.97	8.69	11.63	13.36
									Run 8609181225												
1225-1231	6	0.59	0.061	0.25	0.10	2.11	1.16	0.15	6.44	7.08	2.66	0.67	2.27	12.00	3.20	0.64	0.87	1.03	6.95	9.68	11.85
1231-1237	6	0.62	0.049	0.22	-0.81	2.71	0.92	0.09	7.44	12.93	3.60	0.76	2.44	16.00	3.40	0.66	0.84	0.90	8.25	11.85	14.95
1237-1243	6	0.60	0.079	0.28	1.20	5.82	1.65	0.11	7.15	10.25	3.20	0.90	3.15	17.00	3.20	0.66	0.88	1.18	7.82	11.06	13.60
1243-1249	6	0.58	0.094	0.31	0.74	4.10	1.47	0.08	6.31	6.39	2.53	0.88	3.03	13.00	3.20	0.66	0.89	1.26	6.79	9.26	11.96
1225-1231	7	0.60	0.058	0.24	0.21	2.17	1.18	0.18	6.52	8.80	2.97	0.80	2.76	14.80	3.20	0.65	0.88	1.03	7.15	10.07	12.85
1231-1237	7	0.65	0.054	0.23	-0.27	1.81	1.01	0.18	7.65	9.86	3.14	0.51	2.43	15.20	3.40	0.69	0.89	0.98	8.26	11.27	13.95
1237-1243	7	0.64	0.090	0.30	0.99	4.11	1.53	0.20	7.14	11.93	3.45	1.36	4.96	19.60	3.20	0.70	0.96	1.34	7.92	11.02	15.45
1243-1249	7	0.55	0.065	0.26	1.02	5.44	1.45	0.10	6.06	8.32	2.88	1.37	4.20	15.20	3.20	0.60	0.80	1.05	6.70	9.41	13.04
1225-1231	8	0.58	0.056	0.24	-0.26	1.90	0.95	0.10	7.61	9.86	3.14	0.44	2.45	15.20	3.20	0.62	0.84	0.91	8.22	11.22	13.60
1231-1237	8	0.63	0.046	0.21	-0.06	2.45	1.17	0.22	7.64	12.11	3.48	0.64	2.38	14.80	3.40	0.66	0.85	0.98	8.38	11.65	14.70
1237-1243	8	0.58	0.039	0.20	-0.11	1.97	0.91	0.18	7.24	7.04	2.65	0.68	3.00	13.60	3.20	0.61	0.81	0.89	7.70	10.26	13.30
1243-1249	8	0.58	0.077	0.28	0.10	1.97	1.24	0.11	6.89	9.19	3.03	0.77	2.64	15.00	3.20	0.64	0.89	1.02	7.52	10.51	12.92

(Continued)

* H = Mean wave height; Var(H) = Variance in wave height relative to mean; S(H) = Standard deviation in wave height; Skew(H) = Skewness of wave height elevations relative to mean; Kurt(H) = Kurtosis of wave height elevations relative to mean; Hmax = Maximum wave height; Hmin = Minimum wave height; T = Mean wave period; Var(T) = Variance in wave period relative to mean; S(T) = Standard deviation in wave period; Skew(T) = Skewness of wave period relative to mean; Kurt(T) = Kurtosis of wave period relative to mean; Tmax = Maximum wave period; Tmin = Minimum wave period; Hrms = Root-mean-square wave height; Hs = Average of highest one-third wave heights; H10 = Average of the highest one-tenth wave heights; Trms = Root-mean-square wave period; Ts = Average of the highest one-third wave periods; T10 = Average of highest one-tenth wave periods.

(Sheet 1 of 3)

Table 5 (Continued)

Time EDST	Photo-pole	H m	Var(H) m²	S(H) m	Skew(H)	Kurt(H)	Hmax m	Hmin m	T sec	Var(T) sec	S(T) sec	Skew(T)	Kurt(T)	Tmax sec	Tmin sec	Hrms m	Hs m	H10 m	Trms sec	Ts sec	T10 sec
1225-1231	9	0.58	0.053	0.23	0.02	2.21	1.04	0.15	6.87	7.95	2.82	0.64	2.52	13.80	3.20	0.62	0.84	0.99	7.42	10.20	12.75
1231-1237	9	0.62	0.059	0.24	0.08	2.05	1.12	0.18	7.73	8.47	2.91	0.16	2.19	14.60	3.20	0.66	0.89	1.06	8.25	11.00	12.95
1237-1243	9	0.56	0.040	0.20	-0.09	1.86	0.85	0.12	7.31	9.89	3.14	0.81	2.94	16.00	3.20	0.59	0.79	0.84	7.95	11.09	14.10
1243-1249	9	0.62	0.073	0.27	0.12	1.97	1.12	0.15	7.68	7.56	2.75	0.23	2.03	13.60	3.60	0.67	0.93	1.08	8.15	10.76	12.60
										Run 8609181453											
1453-1459	6	0.49	0.024	0.15	0.18	2.60	0.81	0.14	7.12	9.90	3.15	0.78	2.35	14.40	3.40	0.51	0.67	0.77	7.73	11.13	13.4
1459-1505	6	0.49	0.029	0.17	0.34	2.79	0.94	0.15	7.29	16.28	4.03	1.03	3.41	18.80	3.20	0.52	0.68	0.83	8.32	12.06	16.50
1505-1511	6	0.44	0.025	0.16	0.28	2.69	0.87	0.13	7.02	8.57	2.93	0.83	2.78	14.00	3.20	0.47	0.61	0.74	7.59	10.50	13.50
1511-1517	6	0.46	0.021	0.15	0.23	2.78	0.81	0.14	7.90	17.54	4.19	1.21	5.01	23.40	3.20	0.48	0.62	0.74	8.92	12.64	16.45
1453-1459	7	0.52	0.035	0.19	-0.16	1.88	0.85	0.15	6.24	6.85	2.62	0.97	3.09	13.20	3.20	0.55	0.74	0.80	6.76	9.39	12.00
1459-1505	7	0.49	0.037	0.19	-0.01	1.96	0.89	0.15	6.54	7.73	2.78	0.79	2.79	14.20	3.20	0.53	0.70	0.80	7.10	9.80	12.32
1505-1511	7	0.56	0.043	0.21	0.18	2.52	1.08	0.18	7.40	8.21	2.86	0.35	2.26	13.80	3.20	0.59	0.78	0.94	7.92	10.55	13.15
1511-1517	7	0.55	0.050	0.22	-0.48	2.13	0.90	0.11	7.15	11.09	3.33	0.63	2.35	16.00	3.20	0.58	0.76	0.84	7.87	11.21	13.75
1453-1459	8	0.55	0.038	0.20	0.06	2.00	0.95	0.24	6.89	7.97	2.82	0.84	3.34	15.20	3.20	0.59	0.77	0.90	7.43	10.13	12.80
1459-1505	8	0.51	0.026	0.16	-0.35	1.95	0.76	0.19	7.93	10.97	3.31	0.30	2.09	16.20	3.20	0.54	0.68	0.74	8.58	11.79	13.50
1505-1511	8	0.50	0.052	0.23	0.14	2.18	0.97	0.07	6.26	7.47	2.73	0.80	2.83	13.80	3.20	0.55	0.76	0.91	6.82	9.49	12.04
1511-1517	8	0.55	0.041	0.20	-0.26	2.60	1.04	0.11	7.70	10.34	3.22	0.31	2.07	14.60	3.20	0.59	0.75	0.88	8.33	11.47	13.50
1453-1459	9	0.55	0.046	0.22	0.38	2.39	1.12	0.21	6.73	6.23	2.50	0.23	1.83	12.00	3.20	0.59	0.81	0.95	7.17	9.69	11.10
1459-1505	9	0.48	0.036	0.19	0.02	1.98	0.89	0.14	7.32	8.55	2.92	0.30	2.16	14.60	3.20	0.52	0.69	0.80	7.87	10.65	12.65
1505-1511	9	0.55	0.062	0.25	0.22	2.15	1.10	0.14	7.35	8.88	2.98	0.36	2.15	13.60	3.20	0.61	0.83	1.01	7.92	10.69	13.05
1511-1517	9	0.55	0.048	0.22	-0.27	2.12	0.91	0.10	7.59	8.40	2.90	0.37	2.43	14.40	3.20	0.59	0.78	0.89	8.11	10.93	13.15
										Run 8609201045											
1045-1051	5	0.41	0.016	0.13	-0.57	2.20	0.58	0.12	9.47	15.03	3.88	0.43	2.10	18.20	4.20	0.42	0.53	0.56	10.21	14.04	16.40
1051-1057	5	0.48	0.046	0.22	0.71	2.60	1.01	0.16	9.33	13.89	3.73	0.26	2.03	17.80	3.80	0.52	0.74	0.93	10.03	13.78	16.20
1057-1103	5	0.53	0.066	0.26	0.33	1.78	1.00	0.18	8.89	21.07	4.59	1.90	7.96	27.60	3.60	0.59	0.84	0.99	9.98	13.77	20.00
1103-1109	5	0.63	0.066	0.26	-0.19	1.89	1.10	0.14	9.02	10.57	3.25	0.50	2.63	17.60	3.80	0.68	0.91	1.02	9.57	12.71	15.40
1109-1115	5	0.67	0.084	0.29	-0.21	1.86	1.22	0.15	8.14	9.56	3.09	0.77	2.57	16.20	4.00	0.73	0.98	1.12	8.69	11.97	14.20
1115-1121	5	0.77	0.083	0.29	-0.55	1.95	1.14	0.17	9.34	10.67	3.27	0.09	2.16	16.40	3.20	0.82	1.05	1.12	9.88	13.08	15.07
1121-1127	5	0.53	0.058	0.24	0.49	2.49	1.08	0.14	8.01	12.57	3.55	0.51	1.89	15.20	3.40	0.58	0.80	1.01	8.75	12.46	14.60
1127-1133	5	0.67	0.076	0.28	-0.19	1.67	1.09	0.16	8.86	12.43	3.53	0.28	2.19	16.60	3.80	0.72	0.97	1.05	9.52	12.89	15.35
1045-1051	6	0.59	0.060	0.24	-0.23	1.89	1.07	0.16	7.59	8.80	2.97	0.23	1.61	13.60	3.20	0.64	0.84	0.95	8.13	11.09	12.50
1051-1057	6	0.56	0.061	0.25	0.16	1.87	1.13	0.19	7.72	9.18	3.03	0.29	1.93	14.80	3.60	0.61	0.83	0.97	8.28	11.15	13.10
1057-1103	6	0.55	0.058	0.24	-0.01	1.81	1.00	0.11	9.05	12.30	3.51	0.51	2.68	18.60	3.40	0.60	0.82	0.96	9.69	13.02	16.07
1103-1109	6	0.45	0.040	0.20	-0.02	1.88	0.80	0.06	7.83	9.73	3.12	0.66	3.40	17.40	3.20	0.49	0.68	0.77	8.41	11.17	14.25
1109-1115	6	0.56	0.067	0.26	0.12	1.65	1.02	0.15	7.60	12.99	3.60	0.83	2.64	15.80	3.20	0.61	0.86	0.98	8.40	11.88	15.25
1115-1121	6	0.55	0.049	0.22	-0.35	1.68	0.95	0.19	8.39	11.45	3.38	0.32	2.14	17.00	3.40	0.59	0.77	0.84	9.03	12.23	14.30
1121-1127	6	0.47	0.035	0.19	0.11	1.86	0.84	0.15	9.03	20.02	4.47	0.72	2.55	19.80	3.40	0.50	0.68	0.78	10.05	14.26	18.60
1127-1133	6	0.57	0.070	0.27	-0.31	1.42	0.89	0.13	9.11	16.23	4.03	0.08	1.71	16.60	3.20	0.63	0.84	0.89	9.94	13.85	15.60

(Continued)

Table 5 (Concluded)

Run 8609201500

Time EDST	Photo-pole	H m	Var(H) m²	S(H) m	Skew(H)	Kurt(H)	Hmax m	Hmin m	T sec	Var(T) sec²	S(T) sec	Skew(T)	Kurt(T)	Tmax sec	Tmin sec	Hrms m	Hs m	H10 m	Trms sec	Ts sec	T10 sec
1500-1506	8	0.63	0.040	0.20	-0.58	2.51	0.98	0.20	9.86	12.28	3.50	-0.12	2.33	16.80	3.20	0.66	0.83	0.91	10.44	13.62	15.80
1506-1512	8	0.51	0.050	0.22	0.20	1.72	0.91	0.13	7.09	9.70	3.11	0.38	1.92	14.00	3.20	0.56	0.78	0.88	7.73	10.84	12.85
1512-1518	8	0.54	0.061	0.25	-0.29	1.66	0.90	0.05	8.11	13.81	3.72	0.25	1.92	17.00	3.20	0.59	0.80	0.88	8.90	12.49	14.25
1518-1524	8	0.63	0.040	0.20	-0.58	2.51	0.98	0.20	9.86	12.28	3.50	-0.12	2.33	16.80	3.20	0.66	0.83	0.91	10.44	13.62	15.80
1524-1530	8	0.55	0.038	0.19	-0.22	2.10	0.89	0.14	8.32	15.20	3.90	0.52	2.34	17.00	3.40	0.58	0.76	0.85	9.17	12.86	16.05
1530-1536	8	0.60	0.041	0.20	-1.00	3.27	0.92	0.06	9.50	17.12	4.14	0.40	2.44	19.80	3.20	0.63	0.77	0.86	10.34	14.18	17.73
1536-1542	8	0.60	0.058	0.24	-0.59	2.41	1.02	0.06	9.02	13.57	3.68	0.13	1.80	15.60	3.20	0.64	0.83	0.95	9.72	13.31	15.13
1542-1548	8	0.54	0.071	0.27	-0.06	1.75	0.96	0.07	7.77	10.16	3.19	0.73	3.02	16.00	3.20	0.60	0.84	0.94	8.39	11.27	14.70
1500-1506	9	0.63	0.067	0.26	-0.21	2.26	1.09	0.15	9.84	10.09	3.18	-0.34	2.05	14.20	3.20	0.68	0.92	1.04	10.33	13.46	14.07
1506-1512	9	0.51	0.041	0.20	0.02	1.67	0.83	0.15	7.29	8.63	2.94	0.10	1.92	13.60	3.20	0.54	0.75	0.80	7.85	10.59	12.40
1512-1518	9	0.55	0.054	0.23	-0.07	1.89	1.04	0.14	8.31	13.73	3.70	0.46	2.53	18.00	3.20	0.59	0.79	0.92	9.08	12.43	15.45
1518-1524	9	0.49	0.047	0.22	0.34	2.15	0.97	0.11	8.60	18.28	4.28	0.65	2.53	19.20	3.20	0.53	0.74	0.88	9.58	13.85	16.65
1524-1530	9	0.53	0.029	0.17	-0.03	2.46	0.89	0.19	9.39	14.31	3.78	0.01	1.92	16.80	3.20	0.55	0.71	0.84	10.10	13.72	15.73
1530-1536	9	0.61	0.040	0.20	-0.16	2.27	0.98	0.21	10.09	14.59	3.82	-0.20	1.66	16.60	3.20	0.64	0.82	0.95	10.77	14.18	15.80
1536-1542	9	0.62	0.047	0.22	-0.70	2.54	0.97	0.15	9.58	10.81	3.29	-0.25	2.10	15.20	3.20	0.66	0.83	0.92	10.12	13.15	14.60
1542-1548	9	0.52	0.050	0.22	0.04	2.04	0.99	0.11	7.52	9.01	3.00	0.48	2.39	14.60	3.20	0.57	0.77	0.91	8.08	11.04	13.55

DIST FROM SEABED TO MID-STREAMER (cm)

NOZZLE FLUX (g/cm2/min)

—•— SHOREWARD TRAP   —*— SEAWARD TRAP
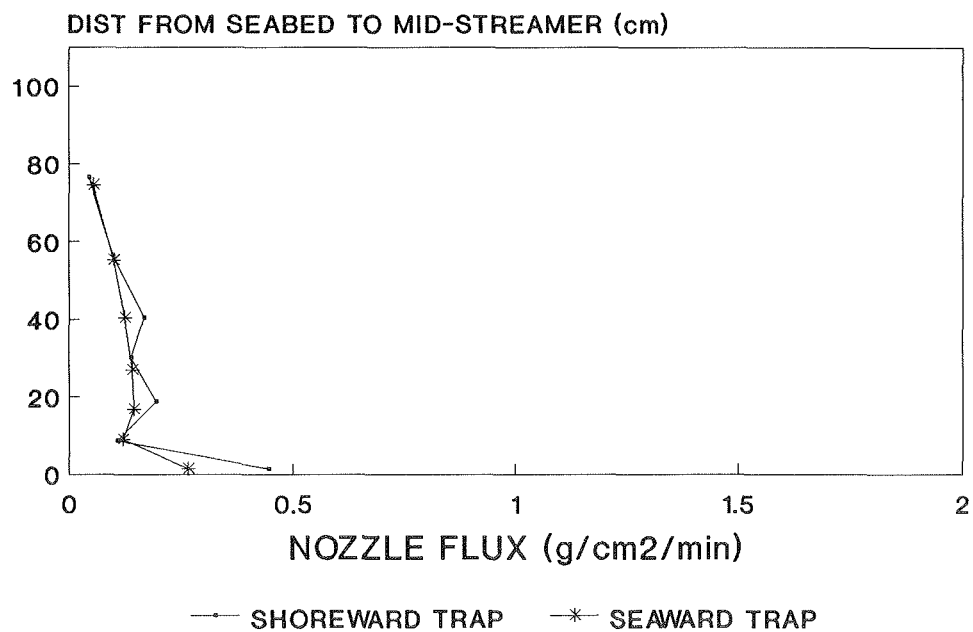
Figure 11. Consistency run 8609160922

DIST FROM SEABED TO MID-STREAMER (cm)

NOZZLE FLUX (g/cm2/min)

—•— SHOREWARD TRAP   —*— SEAWARD TRAP
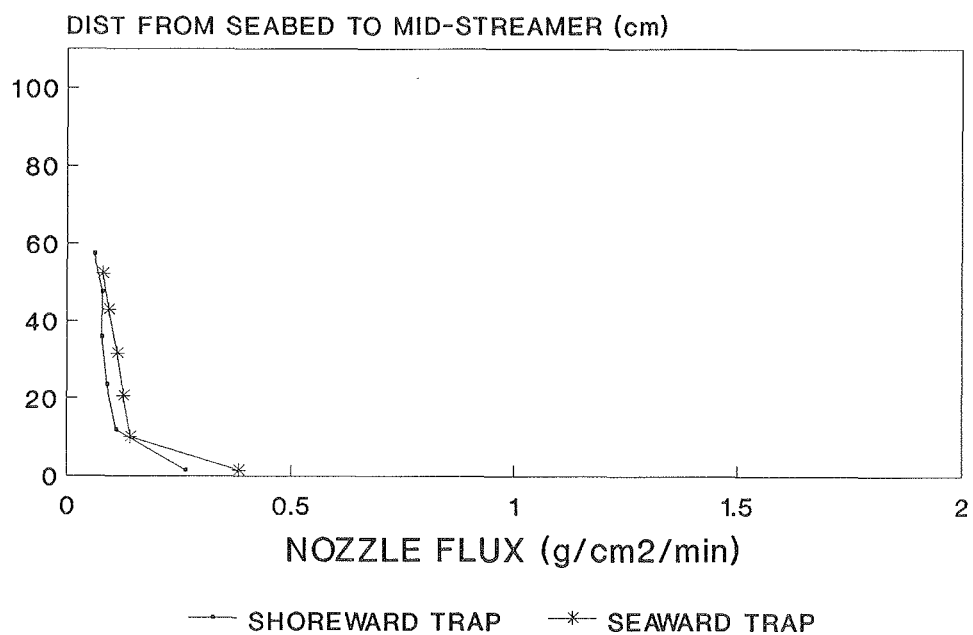
Figure 12. Consistency run 8609160945

DIST FROM SEABED TO MID-STREAMER (cm)

NOZZLE FLUX (g/cm2/min)

—•— SHOREWARD TRAP   —*— SEAWARD TRAP
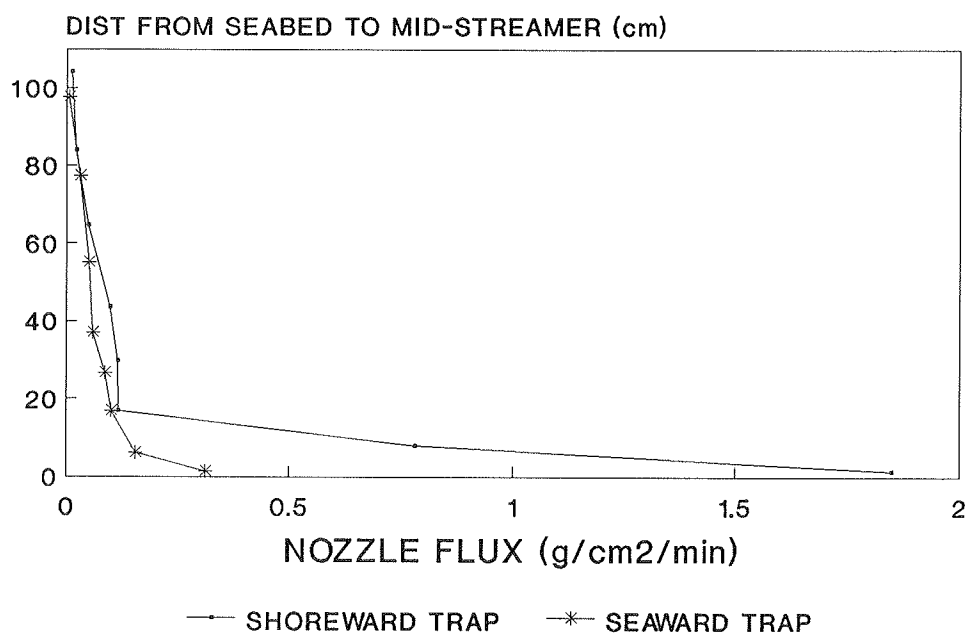
Figure 13.   Consistency run 8609201500-1

DIST FROM SEABED TO MID-STREAMER (cm)

NOZZLE FLUX (g/cm2/min)

—•— SHOREWARD TRAP   —*— SEAWARD TRAP
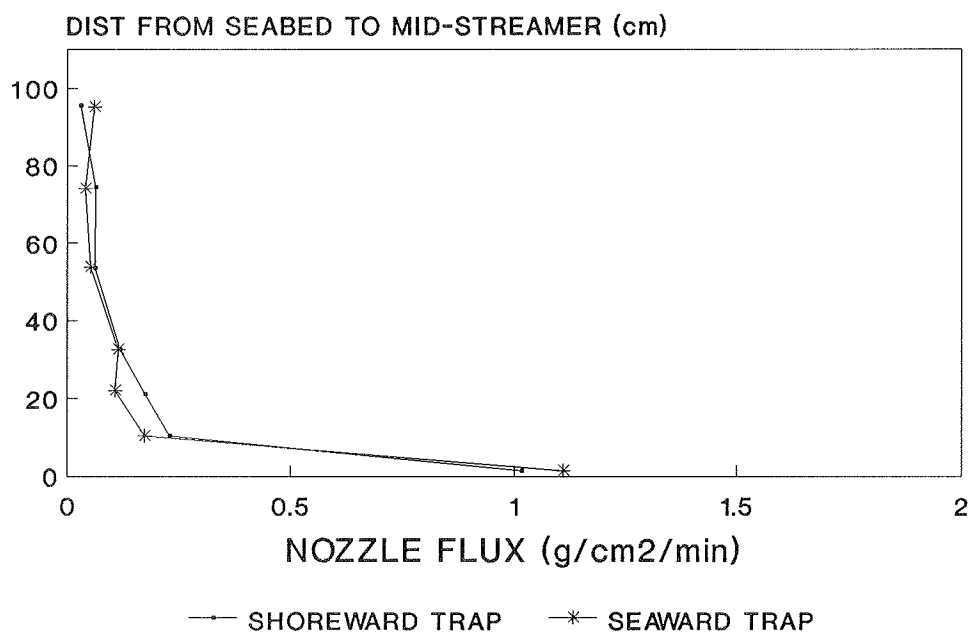
Figure 14.   Consistency run 8609201500-2

DIST FROM SEABED TO MID-STREAMER (cm)
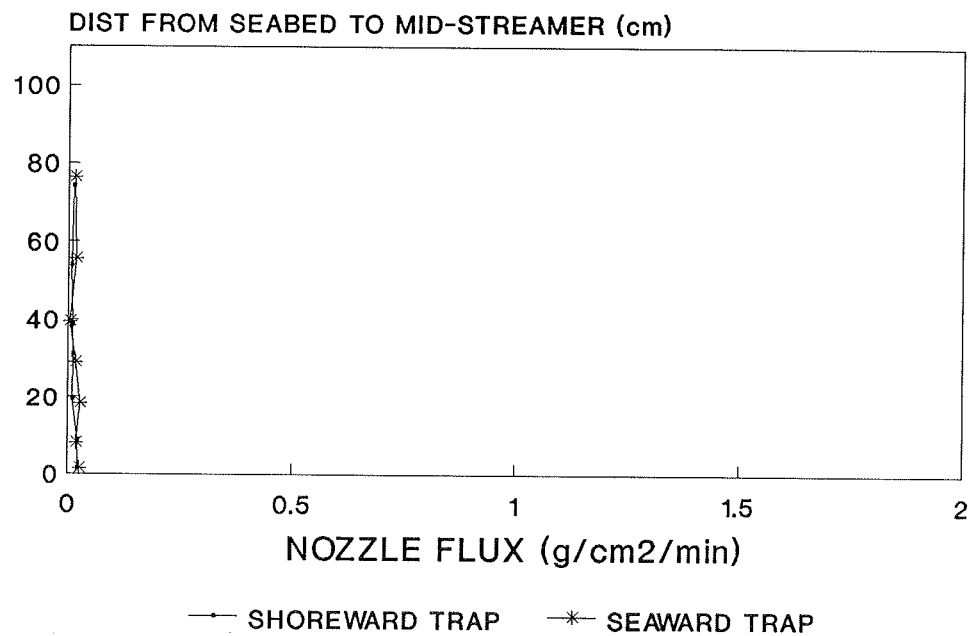
Figure 15. Consistency run 8609211046

DIST FROM SEABED TO MID-STREAMER (cm)
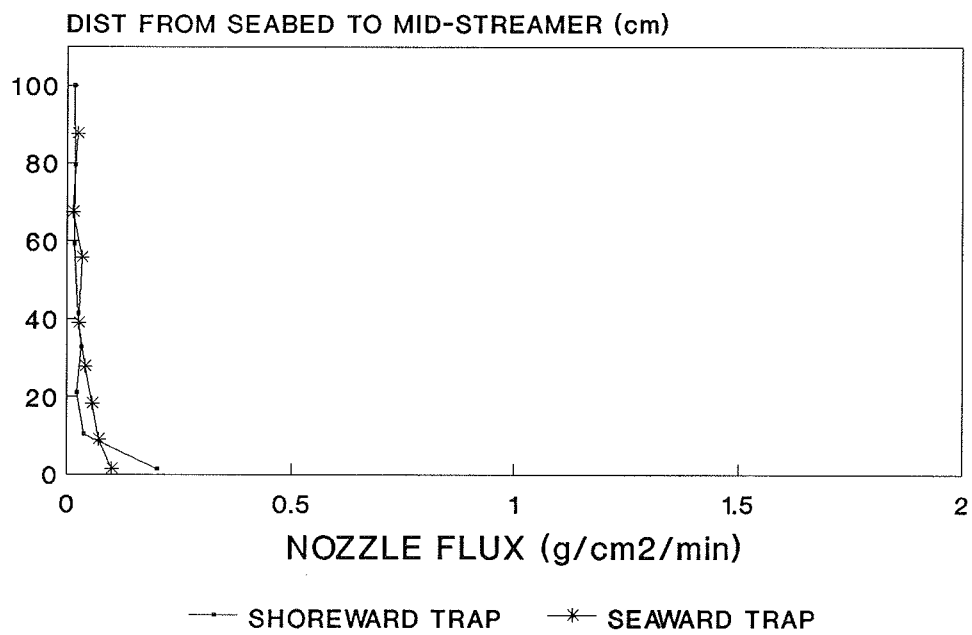
Figure 16. Consistency run 8609211345-1

DIST FROM SEABED TO MID-STREAMER (cm)

— SHOREWARD TRAP   —*— SEAWARD TRAP
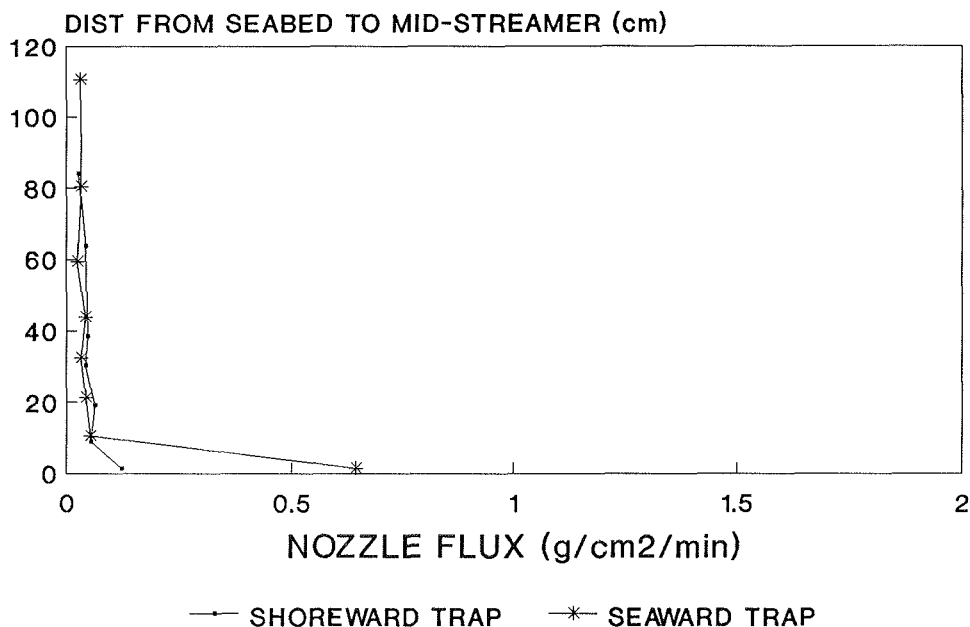
Figure 17. Consistency run 8609211345-2

Kraus, Gingerich, and Rosati 1989). However, wave conditions were different, with clean swell occurring during DUCK85 and more choppy wind waves during SUPERDUCK. The greatest discrepancy in fluxes in Figures 11 through 17 occurred at the bottom streamer and was probably a result of small differences in the angle of alignment or elevation, which would cause sediment to pass under the lower lip of the streamer nozzle.

42. Rosati and Kraus (1989) evaluated trap consistency by comparing the transport rate density and the shape of the vertical flux distribution measured with the shoreward and seaward traps. The longshore transport rate density i is defined as the total immersed weight of transported material crossing a unit length of a shore-normal line per unit time. Consistency ratios, calculated by dividing the lower value of the transport rate density for a particular run (seaward or shoreward trap) by the higher value for a particular run (seaward or shoreward trap) and then multiplying by 100, ranged from 50 to 100 percent for the SUPERDUCK consistency runs. The vertical distributions of sand flux for the consistency data sets were fit with linear,

exponential, and power-law equations. Of the 14 pairs of vertical consistency test sand flux distributions, 10 had the highest squared correlation coefficients with a power-law fit, three were best fit with an exponential relationship, and one was best described linearly. The majority (5 out of 7) of the shoreward and seaward consistency test data sets had similar coefficients and were described by the same type of equation. These favorable comparisons between the transport rate densities and the form of the vertical flux distributions between two closely spaced traps suggests that the streamer trap and nozzles are consistent and provide reproducible time-integrated measurements of the transport rate.

Temporal Sampling Method (TSM) runs

43. Thirty-nine transport rate densities measured in six SUPERDUCK TSM runs for which wave data were available (see Table 2) were used to obtain a relationship for the transport rate density

$$i = \kappa [\rho g \, H_{rms} \, V \, (1 + \alpha \, \frac{dH_{rms}}{dx} + \beta \, \frac{\sigma_v}{V}) + const.] \tag{4}$$

where

κ = empirical coefficient

ρ = density of seawater

g = acceleration due to gravity

V = mean longshore current

α = empirical coefficient

β = empirical coefficient

dH_{rms}/dx = local cross-shore gradient of wave height

Root-mean-square (rms) wave height was used because correlations were always slightly higher with rms wave height than with significant wave height.

44. Standard formulas for the transport rate density i derived from either a bottom shear stress approach (e.g., Komar 1971) or a wave energetics approach (e.g., Inman and Bagnold 1963) reduce to a leading dependence on the product of wave height and longshore current speed if linear shallow-water wave theory is employed. Thus, as a first step, Kraus, Gingerich, and Rosati (1988) plotted measured transport rate densities with respect to the quantity $\rho g H_{rms} V$. The result is shown in Figure 18, in which the straight line is a
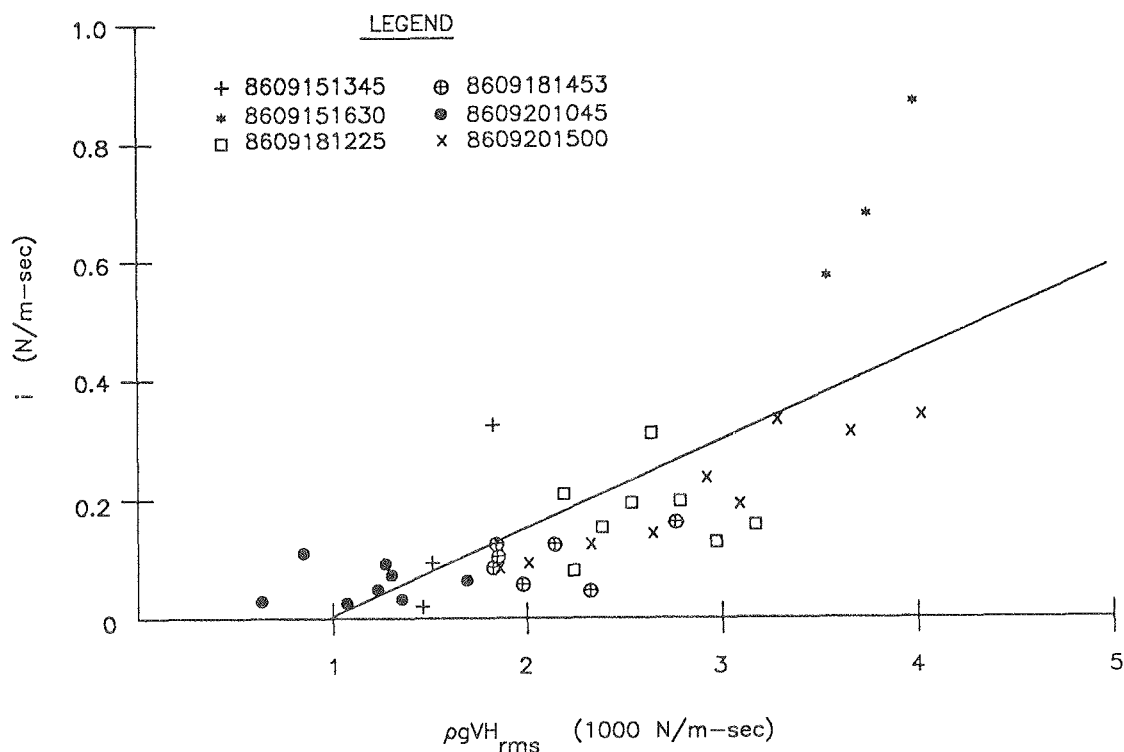
Figure 18. Longshore sand transport rate density versus $H_{rms}V$

best fit from linear regression analysis. Values of the determined regression equation coefficients and the correlation coefficient squared (r^2) are listed in Table 6. Figure 18 shows that the measured transport rate densities are fairly well described by a purely linear function of $H_{rms}V$. However, scatter is relatively great, suggesting that the transport rate densities may have a power-law dependence on $H_{rms}V$, based on the trend of the data.

45. Qualitative observations made during DUCK85 indicated that the trapped amount of sand depended on the intensity of water agitation occurring at or immediately seaward of a trap. For example, the transport rate appeared to increase in turbulent white water as compared with calmer green water for traps located at approximately the same depth. The white, agitated water was produced by waves breaking at the trap or convected to the trap by waves breaking immediately seaward. The local gradient of the wave height dH_{rms}/dx was identified as a readily evaluated measure of water agitation, and the SUPERDUCK TSM runs were configured to provide this quantity. The gradient of wave height was calculated from the nearest two photopoles (i.e., over a 6-m interval). The gradient was usually positive, indicating a decrease in wave

45

Table 6

Summary of Regression Results for Longshore Sand

Transport Rate Density Equation

Expression	κ (10^4)	α	β	Const. N/(m - sec)	r^2
$H_s V$	1.8	0	0	$-1.2(10^3)$	0.45
$H_{rms} V$	2.5	0	0	$-9.9(10^2)$	0.51
$H_{rms} V(1 + \alpha dH_{rms}/dx)$	2.0	20	0	$-7.7(10^2)$	0.66
$H_{rms} V(1 + \alpha dH_{rms}/dx + \beta\sigma_v/V)$	1.5	20	1.8	$-2.4(10^3)$	0.77

height or energy dissipation as the waves moved toward shore. However, in some cases the gradient was negative, indicating that broken waves were reforming.

46. Kraus, Gingerich, and Rosati (1988) introduced the gradient of wave height as a correction to the quantity $H_{rms} V$ in the form of $H_{rms} V(1 + \alpha\ dH_{rms}/dx)$ in which the value of the empirical coefficient α was determined by iteration to provide the best linear least squares fit. The resultant plot and regression line are given in Figure 19. Visual agreement and the correlation coefficient are considerably improved over Figure 18, which involved only the product $H_{rms} V$.

47. The longshore current speed used in the analysis is the average of a time-varying flow. The sand transport rate should depend on the range of current speed as well as the average. As a measure of the range, Kraus, Gingerich, and Rosati (1988) chose the coefficient of variation of the current speed σ_v/V , in which σ_v is the standard deviation of the speed during the averaging interval. The coefficient of variation was conceptualized as providing a correction to the leading term $H_{rms} V$, and the quantity $H_{rms} V(1 + \alpha\ dH_{rms}/dx + \beta\ \sigma_v/V)$ was used for regression. The result is shown in Figure 20, and associated values of determined coefficients are given in Table 6. Grouping of the data points about the regression line is improved over previous plots, and the apparent necessity of using a nonlinear or power law function of $H_{rms} V$, as was suggested by Figure 18, is eliminated.
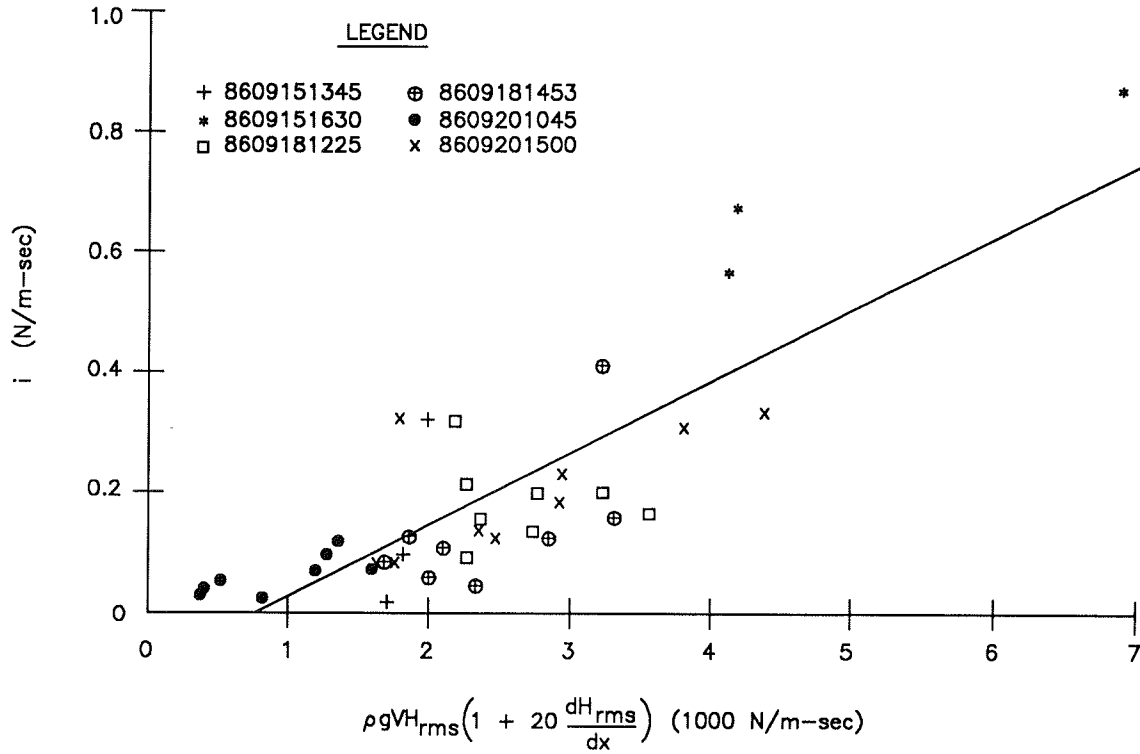
Figure 19. Longshore sand transport density versus
$H_{rms}V(1 + \alpha \ dH_{rms}/dx)$
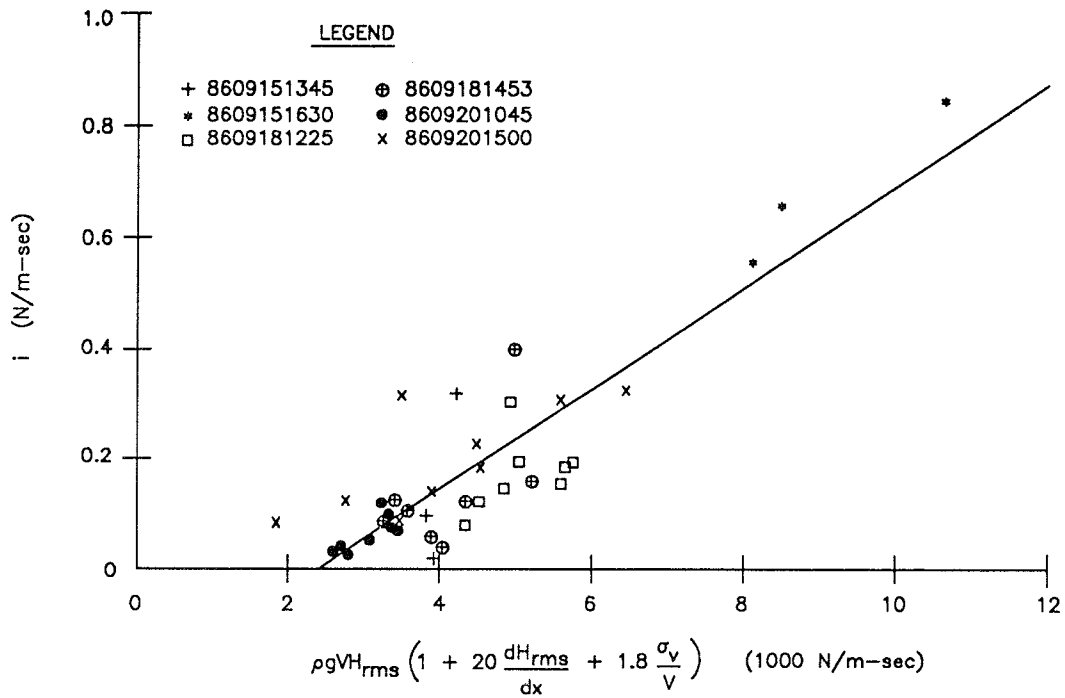
Figure 20. Longshore sand transport rate density versus
$H_{rms}V(1 + \alpha \ dH_{rms}/dx + \beta \ \sigma_v/V)$

47

48. The correlation lines in Figures 18, 19, and 20 all intercept the positive x-axis (the term "const." in Equation 4). The value of the intercept is partially an artifact of the use of a straight-line regression analysis. However, the intercept may be interpreted as an effective cutoff for transport of significance in engineering applications, since transport rates lying below this value evidently have a much weaker dependence on the quantity $H_{rms}V$ than the plotted measured values.

49. Stepwise correlation analysis indicated that there was no relation between the quantities H_{rms} , dH_{rms}/dx , V , and σ_v . In a situation where the longshore current is produced by obliquely incident waves, the magnitude of the current speed is proportional to the square root of the wave height. In the present case, V and H_{rms} were not related because the experiments were performed in or near the feeder current of a rip current. Caution should be taken in general use of the correction term proportional to α , as most TSM measurements were performed on a plateau with a very mild slope. Values of dH_{rms}/dx ranged from -0.035 to 0.037 and values of σ_v/V ranged from 0.07 to 2.03. Use of the relationship with the two correction terms requires detailed knowledge of wave height and current characteristics, and may be applicable only if these data are available.

PART IV: CONCLUDING DISCUSSION

50.   Previous field data collection efforts aimed at making direct point measurements of longshore sand transport in the surf zone have either measured the suspended sand concentration, from which a rate must be inferred by taking the product with a longshore current speed, or have used traps to measure only bed-load transport.   Neither of these two methods taken individually provides the total transport rate.   The SUPERDUCK surf zone experiment described in this report successfully measured the longshore sand flux through the water column as it varied with time at one or two points in the surf zone.

51.   The portable streamer traps developed in this project were found to give reliable and consistent results by comparison of sand fluxes obtained with traps placed close to each other.   The consistency ratio, calculated by dividing the lower value of the transport rate density for a particular run by the higher value for that run and multiplying by 100, ranged from 50 to 100 percent for the SUPERDUCK consistency tests.   Of the 14 vertical distributions of sand flux, the majority of the shoreward and seaward consistency test data sets had similar coefficients and were described by a power-law equation. These favorable comparisons between magnitudes of the transport rate densities and the shape of the vertical flux distributions obtained at two closely spaced traps indicate that the streamer trap and nozzles are indeed consistent and provide reproducible measurements of the transport rate.

52.   The transport rate density measured at SUPERDUCK was found to be closely related to the product of wave height and longshore current speed, consistent with previously derived theoretical models of transport.   The correlation was considerably improved, however, by including corrections due to energy dissipation introduced by breaking waves and the variation in the longshore current speed.

REFERENCES

Birkemeier, W. A., Baron, C. F., Leffler, M. A., Hathaway, K. K., Miller, H. C., and Strider, J. B. 1989. "SUPERDUCK Nearshore Processes Experiment Data Summary CERC Field Research Facility," Miscellaneous Paper CERC-89-16, US Army Engineer Waterways Experiment Station, Coastal Engineering Research Center, Vicksburg, MS.

Byrnes, M. R. 1989. "SUPERDUCK Beach Sediment Sampling Experiment, Report 1: Data Summary and Initial Observations," Miscellaneous Paper CERC-89-18, US Army Engineer Waterways Experiment Station, Coastal Engineering Research Center, Vicksburg, MS.

Crowson, R. A., Birkemeier, W. A., Klein, H. M., and Miller, H. C. 1988. "SUPERDUCK Nearshore Processes Experiment: Summary of Studies, CERC Field Research Facility," Technical Report CERC-88-12, US Army Engineer Waterways Experiment Station, Coastal Engineering Research Center, Vicksburg, MS.

Ebersole, B. A., and Hughes, S. A. "SUPERDUCK Photopole Experiment," Miscellaneous Paper in preparation, US Army Engineer Waterways Experiment Station, Coastal Engineering Research Center, Vicksburg, MS.

Field Research Facility. 1986 (Sep). "Preliminary Data Summary," Monthly Series, US Army Engineer Waterways Experiment Station, Coastal Engineering Research Center, Vicksburg, MS.

Friedman, G. M., and Johnson, K. G. 1982. Exercises in Sedimentology, Wiley, New York.

Hughes, S. A., Kraus, N. C., and Richardson, T. W. 1987. "SUPERDUCK - A Nearshore Process Field Experiment," (video), CERC File No. 87057B, 21Jul87, Log #6209, 24 min.

Inman, D. L., and Bagnold, R. A. 1963. "Littoral Processes," In: M. N. Hill, Ed., The Sea, Interscience, New York, pp 529-533.

Katori, S. 1982. "Measurement of Sediment Transport by Streamer Trap," Report of the 6th Cooperative Field Investigation, Report No. 16, TR-81-2, Nearshore Environment Research Center, Tokyo, Japan, pp 138-141. (in Japanese)

_____. 1983. "Measurement of Sediment Transport by Streamer Trap," Report of the 7th Cooperative Field Investigation, Report No. 17, TR-82-2, Nearshore Environment Research Center, Tokyo, Japan, pp 110-117. (in Japanese)

Komar, P. D. 1971. "The Mechanics of Sand Transport on Beaches," Journal of Geophysical Research, Vol 76, No. 3, pp 713-721.

Kraus, N. C. 1987. "Application of Portable Traps for Obtaining Point Measurements of Sediment Transport Rates in the Surf Zone," <u>Journal of Coastal Research</u>, Vol 2, No. 2, pp 139-152.

Kraus, N. C., Gingerich, K. J., and Rosati, J. D. 1988. "Toward an Improved Empirical Formula for Longshore Sand Transport," <u>Proceedings, 21st Coastal Engineering Conference</u>, American Society of Civil Engineers, pp 1182-1196.

_____. 1989. "DUCK85 Surf Zone Sand Transport Experiment," Technical Report CERC-89-5, US Army Engineer Waterways Experiment Station, Coastal Engineering Research Center, Vicksburg, MS.

Kraus, N. C., and Nakashima, L. 1986. "Field Method for Determining Rapidly the Dry Weight of Wet Sand Samples," <u>Journal of Sedimentary Petrology</u>, Vol 56, No. 4, pp 550-551.

Rosati, J. D., and Kraus, N. C. 1988. "Hydraulic Calibration of the Streamer Trap," <u>Journal of Hydraulic Engineering</u>, Vol 114, No. 12, pp 1527-1532.

_____. 1989. "Development of a Portable Sand Trap for Use in the Nearshore," Technical Report CERC-89-11, US Army Engineer Waterways Experiment Station, Coastal Engineering Research Center, Vicksburg, MS.

Stauble, D. K., Holem, G. W., Byrnes, M. R., Anders, F., and Meisburger, E. P. "SUPERDUCK Beach Sediment Sampling Experiment, Report 2: Beach Profile Change and Sediment Dynamics," Miscellaneous Paper in preparation, US Army Engineer Waterways Experiment Station, Coastal Engineering Research Center, Vicksburg, MS.

APPENDIX A: DATA

1.   This appendix contains a listing of the basic data collected during the SUPERDUCK surf zone sand transport experiments. Data are given for the following quantities:

a.   Wet weight of collected sand (Table A1).

b.   Elevations of individual trap streamers (Table A2).

c.   Water levels during the experiments (Table A3).

d.   Horizontal coordinates of the photopoles (Field Research Facility (FRF) coordinate system) (Table A4).

e.   Grain size data (Table A5).

2.   Table A1 gives the weight of the sand collected in the streamers as recorded in the field logbooks, without adjustments for trap efficiency. A value of 0.0 indicates that no sand was collected in the streamer, and blank spaces denote no streamer at that elevation. The wet sand was weighed in a drip-free state in small patches of sieve cloth, and the weight of the sieve cloth was subtracted to arrive at the values given in Table A1. The drip-free wet weight (WW) and the dry weight (DW) of samples consisting primarily of sand are linearly related (Kraus and Nakashima 1986[*]) for a wide range of common grain sizes and sample weights as

$$DW = c \ WW \tag{A1}$$

for which the empirical coefficient c must be determined through calibration for the particular field operation and weighing procedure, since judgment of the drip-free state is somewhat subjective. The value c ranged from 0.72 to 0.81 for the SUPERDUCK experiments; an average value obtained from samples analyzed during one run per day was used to convert wet weights to dry weights for samples collected during that day's runs.

3.   Table A2 gives the elevation of each streamer on each trap deployed for a particular run. Elevations are given as distances from the bed to the

---

[*] References cited in Appendix A can be found in the list of references at the end of the main text.

center of the streamer nozzle.

4. Table A3 lists water levels relative to the National Geodetic Vertical Datum (NGVD) recorded at a tide gage located at the end of the FRF pier during the times of six Temporal Sampling Method (TSM) experiment runs. The NGVD is related to Mean Sea Level (MSL) at the FRF by the relation $MSL(m) = NGVD(m) + 0.067$.

5. Table A4 gives the horizontal coordinates of the photopoles in the FRF coordinate system.

6. Table A5 summarizes grain size statistics (calculated using Moment and Folk methods (Friedman and Johnson 1982)) for samples retained from 37 traps representing 11 experiment runs.

Table A1

Sand Wet Weights, g

Trap Number	Streamer Number								
	1	2	3	4	5	6	7	8	9
				Run 8609111745					
1	1554.4	584.4	1992.2	1518.3	1013.4	356.3	28.1		
2	21.1	84.8	33.1	26.2	32.3	25.9	18.3		
3	195.2	52.6	36.7	24.8	17.1	14.7	3.1		
4	216.9	22.3	25.3	20.2	26.1	15.6	10.8	3.1	
5	63.6	45.0	43.8	37.6	25.6	27.4	13.3	6.7	
6	21.5	11.1	6.6	6.3	6.3	5.0	5.4	1.1	
				Run 8609121037					
1	125.8	28.8	76.3	50.6	54.0	37.4	24.1		
2	481.5	79.4	102.2	43.5	51.3	20.3	20.6		
3	834.2	142.5	62.7	29.6	14.6	9.9	4.6		
4	378.4	50.3	37.9	32.0	33.8	19.5	1.0	1.2	
5	94.0	65.9	68.8	50.4	33.9	33.5	18.8	8.8	
6	102.9	150.3	17.3	38.1	24.1	17.4	9.7	8.7	
				Run 8609151345					
1	51.0	28.1	24.2	22.2	14.1	4.6	4.6		
2	28.7	16.9	16.7	17.0	17.9	11.5	19.5		
3	177.5	103.4	88.1	139.3	76.0	14.1	1.8		
4	41.8	40.2	22.4	9.2	24.5	12.3	15.1	8.5	
5	884.9	360.1	305.7	227.3	124.9	48.2	7.5	4.0	
6	55.1	31.3	27.8	20.9	29.3	22.1	17.1	14.2	
				Run 8609151630					
1	1655.5	391.5	447.7	269.7	101.8	18.1	3.5		
2	1431.8	537.7	717.0	553.2	316.9	2.5	21.2	9.8	
3	2641.3	717.2	608.9	457.9	374.2	236.8	69.6	18.6	
				Run 8609160922					
1	148.5	52.3	94.0	67.1	81.6	47.7	21.5		
2	89.1	58.7	70.6	68.5	60.5	48.5	26.3		
				Run 8609160945					
1	88.5	53.3	43.3	37.4	38.4	28.9			
2	127.9	68.6	60.9	54.6	44.8	38.9			

(Continued)

Trap Number	Streamer Number								
	1	2	3	4	5	6	7	8	9
				Run 8609161116					
1	496.8	356.4	246.1	93.0	25.1	3.9	0.0		
2	542.0	63.2	73.9	43.3	17.3	3.4	7.8		
3	187.3	29.7	51.5	38.1	21.3	1.9	1.5		
4	430.4	112.2	86.5	63.5	58.9	24.3	4.1	1.1	
5	195.2	123.8	105.3	94.7	55.9	24.8	6.4	0.7	
6	643.3	237.1	345.0	308.9	250.3	104.6	18.3	2.1	3.4
7	1793.4	472.1	1054.7	805.2	929.7	253.2	64.4	16.2	7.8
8	1648.1	1549.6	1267.7	1023.4	773.4	461.3	69.7	14.3	
9	18.2	6.5	22.2	10.0	16.1	17.1	7.3		
10	16.9	15.3	16.3	16.8	8.7	8.7	10.7		
				Run 8609181225					
1	268.4	214.6	187.5	149.4	113.2	41.6	8.4		
2	108.6	52.6	63.9	46.7	48.0	25.2	21.9		
3	302.9	80.8	154.9	129.2	74.1	35.4	7.4		
4	318.5	115.0	76.2	51.7	55.0	24.9	23.4	11.6	
5	284.9	156.9	151.8	114.1	95.0	48.0	8.2	7.6	
6	114.8	93.0	98.8	88.2	81.0	48.1	18.5	3.2	
7	500.8	191.7	212.1	160.4	125.3	77.0	13.4	1.2	
8	142.2	139.1	127.1	103.7	92.1	51.5	24.2	7.2	7.1
				Run 8609181453					
1	151.6	98.0	86.7	77.3	65.2	29.8	14.7		
2	69.3	22.7	28.3	26.1	23.5	15.2	8.1		
3	115.5	50.4	82.4	69.6	44.1	27.9	4.5		
4	205.7	45.0	32.3	29.5	28.4	17.4	17.6	5.5	
5	516.9	314.1	287.4	223.7	198.4	145.3	38.7	5.1	
6	105.3	96.0	84.6	85.5	87.9	54.6	45.8	18.0	0.0
7	178.5	48.8	98.8	84.8	62.8	14.9	0.0	3.3	
8	67.6	49.3	43.1	34.8	32.2	24.9	19.3	11.6	
9	381.2	170.2	148.8	124.7	97.5	57.6	14.3		
10	267.4	53.6	45.4	36.7	24.2	25.5	16.8		
				Run 8609191016					
1	698.7	74.0	13.1	0.0	0.9	2.5	8.9	5.3	
2	1418.0	257.2	114.1	39.5	0.3	5.5	13.6	4.1	
3	61.0	53.8	36.6	43.2	42.0	28.1	25.2	20.6	
4	20.6	13.0	19.8	17.4	70.6	21.2	10.8		
5	36.6	25.0	16.7	15.4	6.9	10.9	9.4		
6	86.4	165.9	132.5	86.7	136.4	75.0	79.9		

(Continued)

Trap Number	Streamer Number								
	1	2	3	4	5	6	7	8	9
				Run 8609191230					
1	351.7	283.6	230.0	195.9	166.2	85.1	32.1		
2	119.7	41.4	45.6	35.7	33.7	22.8	26.7	20.0	
3	402.1	234.2	245.2	173.8	109.9	31.3	9.6		
4	377.2	67.5	41.3	36.3	29.4	17.8	3.4		
5	1186.8	93.1	227.3	164.2	129.6	18.8	5.8	3.1	
6	156.1	63.9	43.1	42.9	35.3	25.1	17.9	13.8	4.1
7	339.0	197.2	212.1	176.6	151.3	86.8	22.9	3.6	
8	54.0	32.5	31.0	24.0	19.1	12.1	11.6	6.1	
				Run 8609201045					
1	96.3	101.7	95.4	80.7	80.3	42.2	34.3		
2	116.5	25.9	58.6	49.2	14.4	23.1	18.8	14.5	
3	183.3	11.3	58.0	39.3	32.7	32.6	21.7		
4	65.0	36.8	39.5	38.3	25.6	24.8	19.5		
5	28.3	27.8	28.9	20.5	18.2	23.2	13.0	7.7	
6	36.7	38.4	16.3	30.0	23.2	14.2	6.0	6.7	
7	34.5	19.6	24.0	19.2	19.2	14.3	9.9	6.4	
8	52.0	55.5	55.0	47.8	42.2	30.6	16.9	12.6	
				Run 8609201500					
1	1322.2	269.2	166.3	114.0	81.2	44.9	24.8		
2	496.8	124.9	103.5	75.4	64.2	40.0	11.6	4.1	
3	1003.7	84.1	72.1	40.1	22.9	11.1	2.9		
4	1076.6	210.1	84.6	63.6	34.8	21.4	6.6		
5	368.6	75.0	73.8	50.8	34.3	15.2	4.5	4.1	
6	963.1	174.1	84.3	82.5	43.7	26.7	9.7	2.7	
7	369.2	22.6	33.7	33.4	28.4	14.1	6.2	3.4	
8	62.4	44.8	29.1	24.9	17.1	14.6	8.6	1.9	
9	203.1	66.0	50.7	34.1	17.8	18.5	8.8		
10	222.3	50.7	30.8	33.1	15.1	11.7	17.3		
				Run 8609211046					
1	7.1	10.6	5.4	5.6	5.1	3.6	5.9	4.4	
2	8.8	9.1	13.4	8.6	2.4	8.9	7.4		

(Continued)

Trap	Streamer Number								
Number	1	2	3	4	5	6	7	8	9
				Run 8609211345					
1	16.6	3.6	7.8	4.1	4.4	3.4	4.1		
2	64.0	21.1	9.3	15.6	7.1	3.6	8.6	2.7	
3	37.5	21.5	14.2	9.4	10.4	7.3	5.9		
4	71.6	15.1	9.8	12.2	4.6	4.3	5.9		
5	23.6	10.0	8.8	8.2	8.1	6.5	9.0	4.2	
6	33.3	8.6	16.4	15.2	15.3	9.4	6.9	6.6	4.2
7	40.1	10.9	6.5	9.3	7.2	4.7	5.2	4.8	
8	19.8	20.4	16.4	11.6	7.7	9.9	3.8	6.8	
9	54.0	42.8	23.9	17.2	13.3	10.9	4.6		
10	30.7	21.7	18.1	14.8	11.0	10.0	5.2		
11	24.7	16.0	18.3	12.5	13.9	12.5	7.9		
12	128.8	15.3	12.6	9.9	12.1	7.4	9.5	9.1	
13	97.0	30.8	34.1	22.8	16.7	16.6	38.7		
14	162.9	60.1	47.2	33.2	18.7	15.0	11.2		
15	137.1	28.5	32.1	22.7	22.8	13.7	6.7	4.5	
16	144.5	56.1	28.7	28.6	29.2	20.7	14.9	13.6	11.7
				Run 8609220730					
1	361.3	389.7	430.9	388.8	357.6	250.4	76.7		
2	485.3	321.8	364.6	348.5	322.8	193.9	104.7	36.4	
3	962.9	629.2	682.1	595.4	359.5	289.7	97.0		
4	702.1	514.3	477.5	485.4	349.3	315.9	197.9		
5	665.2	496.3	510.0	421.9	405.3	342.3	209.5	70.8	
6	405.1	360.8	308.4	283.0	255.3	166.1	110.3	61.9	28.4
7	495.8	454.1	419.6	396.1	373.3	218.4	116.8	47.0	
8	361.4	355.4	344.5	333.7	294.4	196.7	91.0	43.4	
				Run 8609221600					
1	194.1	157.5	151.5	142.1	134.8	113.3	61.8		
2	125.5	67.7	44.1	48.5	40.0	29.2	27.0	27.2	
3	206.8	107.1	108.1	89.1	65.5	44.3	15.9		
4	80.0	36.0	41.4	41.5	28.7	36.6	36.2		
5	106.3	73.0	82.4	65.3	61.1	56.3	32.3	15.9	
6	81.7	44.3	27.6	24.0	27.3	20.6	16.1	20.8	9.8
7	141.8	87.2	102.6	93.7	81.9	61.1	36.8	15.0	
8	80.5	52.5	36.1	28.5	24.6	16.9	14.7	6.1	
9	75.1	56.9	45.6	38.4	30.5	23.0	10.6		
10	68.3	38.8	32.5	22.7	22.2	17.1	14.7		

(Continued)

Table A1 (Concluded)

Trap Number	Streamer Number								
	1	2	3	4	5	6	7	8	9

Run 8609221750

Trap Number	1	2	3	4	5	6	7	8	9
1	508.2	563.9	436.9	199.8	61.8	6.0	6.6		
2	1505.8	1338.1	979.3	1026.2	599.7	269.8	35.8		
3	363.3	247.1	281.7	239.8	177.0	80.5	20.7		
4	111.6	31.7	40.3	33.4	23.9	20.8	14.8	5.1	
5	79.2	29.7	24.3	22.1	21.1	22.2	14.3	9.3	
6	26.0	19.5	20.7	28.0	24.4	20.4	17.6	13.8	
7	19.0	27.7	29.4	24.5	47.2	22.3	14.5	11.7	8.1
8	33.9	22.7	29.0	22.3	11.7	17.0	11.9	13.1	
9	57.5	34.8	40.0	37.4	38.4	28.2	17.1		
10	44.6	44.0	36.5	36.6	33.5	22.2	26.2		

Run 8609231035

Trap Number	1	2	3	4	5	6	7	8	9
1	60.3	44.4	19.3	3.6	14.6	11.3	8.8		
2	27.5	22.7	7.2	10.4	6.9	8.9	6.2	6.0	
3	30.0	12.6	13.5	16.0	15.0	7.1	3.2		
4	30.6	38.4	19.7	10.2	9.6	12.3	21.8		
5	70.2	10.2	10.3	3.4	10.3	8.8	3.7	2.0	

Table A2

Streamer Elevations from Local Sea Bottom, m

Trap Number	Streamer Number								
	1	2	3	4	5	6	7	8	9
				Run 8609111745					
1	0.014	0.099	0.210	0.321	0.410	0.537	0.743		
2	0.014	0.095	0.091	0.308	0.403	0.518	0.632		
3	0.014	0.095	0.210	0.305	0.426	0.540	0.743		
4	0.014	0.111	0.206	0.318	0.394	0.530	0.749	0.978	
5	0.014	0.111	0.200	0.324	0.426	0.552	0.756	0.968	
6	0.014	0.108	0.203	0.305	0.397	0.524	0.730	0.943	
				Run 8609121037					
1	0.014	0.105	0.219	0.340	0.451	0.603	0.822		
2	0.014	0.095	0.197	0.311	0.403	0.565	0.762		
3	0.014	0.086	0.197	0.292	0.407	0.559	0.781		
4	0.014	0.099	0.200	0.321	0.429	0.562	0.784	0.981	
5	0.014	0.121	0.203	0.318	0.426	0.603	0.803	1.016	
6	0.014	0.086	0.187	0.286	0.394	0.556	0.769	0.984	
				Run 8609151345					
1	0.014	0.089	0.194	0.301	0.400	0.568	0.775		
2	0.014	0.095	0.187	0.298	0.400	0.553	0.746		
3	0.014	0.092	0.194	0.292	0.410	0.619	0.829		
4	0.014	0.121	0.219	0.340	0.419	0.546	0.768	0.965	
5	0.014	0.111	0.206	0.324	0.432	0.603	0.807	1.022	
6	0.014	0.111	0.210	0.308	0.435	0.588	0.699	0.797	
				Run 8609151630					
1	0.014	0.108	0.213	0.314	0.435	0.648	0.861		
2	0.014	0.121	0.210	0.321	0.403	0.584	0.743	0.908	
3	0.014	0.121	0.238	0.330	0.422	0.552	0.708	0.860	
				Run 8609160922					
1	0.014	0.086	0.187	0.301	0.400	0.565	0.765		
2	0.014	0.089	0.168	0.270	0.400	0.553	0.746		
				Run 8609160945					
1	0.014	0.118	0.235	0.359	0.476	0.575			
2	0.014	0.099	0.200	0.315	0.429	0.524			

(Continued)

Trap	Streamer Number								
Number	1	2	3	4	5	6	7	8	9
				Run 8609161116					
1	0.014	0.095	0.200	0.283	0.384	0.546	0.753		
2	0.014	0.092	0.203	0.314	0.406	0.565	0.753		
3	0.014	0.102	0.203	0.305	0.422	0.600	0.746		
4	0.014	0.121	0.213	0.330	0.410	0.540	0.759	0.911	
5	0.014	0.118	0.206	0.334	0.429	0.556	0.711	0.864	
6	0.014	0.095	0.194	0.314	0.403	0.527	0.686	0.838	1.057
7	0.014	0.111	0.210	0.334	0.441	0.546	0.705	0.861	1.073
8	0.014	0.089	0.197	0.305	0.400	0.530	0.762	0.978	
9	0.014	0.105	0.206	0.327	0.445	0.540	0.768		
10	0.014	0.118	0.226	0.330	0.435	0.537	0.734		
				Run 8609181225					
1	0.014	0.092	0.197	0.312	0.403	0.572	0.776		
2	0.014	0.088	0.200	0.310	0.402	0.561	0.752		
3	0.014	0.096	0.195	0.295	0.410	0.579	0.789		
4	0.014	0.118	0.219	0.326	0.402	0.536	0.746	0.955	
5	0.014	0.115	0.204	0.321	0.426	0.601	0.801	1.007	
6	0.014	0.099	0.191	0.295	0.422	0.549	0.759	0.958	
7	0.014	0.099	0.198	0.315	0.426	0.585	0.792	0.994	
8	0.014	0.092	0.207	0.298	0.403	0.559	0.769	0.978	1.120
				Run 8609181453					
1	0.014	0.108	0.209	0.284	0.395	0.557	0.735		
2	0.014	0.083	0.169	0.251	0.359	0.556	0.744		
3	0.014	0.105	0.210	0.314	0.517	0.844	1.181		
4	0.014	0.118	0.223	0.340	0.413	0.547	0.763	1.080	
5	0.014	0.115	0.204	0.321	0.426	0.607	0.810	1.012	
6	0.014	0.099	0.191	0.311	0.514	0.644	0.854	1.053	1.266
7	0.014	0.124	0.220	0.343	0.512	0.744	0.919	1.150	
8	0.014	0.088	0.210	0.336	0.447	0.562	0.772	0.981	
9	0.014	0.099	0.210	0.324	0.432	0.642	0.855		
10	0.014	0.092	0.203	0.310	0.428	0.625	0.822		
				Run 8609191016					
1	0.014	0.067	0.153	0.279	0.397	0.578	0.791	1.063	
2	0.014	0.111	0.197	0.311	0.467	0.648	0.845	1.051	
3	0.014	0.073	0.143	0.257	0.368	0.587	0.810	1.019	
4	0.014	0.079	0.185	0.346	0.546	0.838	1.146		
5	0.014	0.083	0.194	0.333	0.540	0.750	0.960		
6	0.014	0.096	0.211	0.321	0.524	0.737	0.928		

(Continued)

Trap	Streamer Number								
Number	1	2	3	4	5	6	7	8	9

Run 8609191230

1	0.014	0.064	0.144	0.261	0.360	0.544	0.747		
2	0.014	0.070	0.153	0.263	0.371	0.562	0.756	1.076	
3	0.014	0.080	0.207	0.359	0.543	0.740	0.950		
4	0.014	0.064	0.172	0.311	0.486	0.731	1.042		
5	0.014	0.089	0.232	0.393	0.565	0.788	0.982	1.150	
6	0.014	0.057	0.149	0.256	0.396	0.555	0.711	0.860	1.051
7	0.014	0.080	0.157	0.267	0.382	0.551	0.748	1.008	
8	0.014	0.048	0.140	0.241	0.362	0.626	0.807	0.943	

Run 8609201045

1	0.014	0.069	0.178	0.285	0.409	0.578	0.785		
2	0.014	0.067	0.175	0.295	0.403	0.565	0.753	0.971	
3	0.014	0.080	0.182	0.302	0.496	0.626	0.833		
4	0.014	0.080	0.179	0.305	0.404	0.633	0.843		
5	0.014	0.092	0.200	0.298	0.428	0.574	0.781	0.987	
6	0.014	0.092	0.245	0.403	0.600	0.781	0.991	1.171	
7	0.014	0.080	0.172	0.317	0.425	0.555	0.752	0.958	
8	0.014	0.064	0.179	0.299	0.401	0.554	0.764	0.970	

Run 8609201500

1	0.014	0.071	0.186	0.284	0.424	0.605	0.819		
2	0.014	0.086	0.187	0.308	0.451	0.626	0.867	1.070	
3	0.014	0.095	0.203	0.330	0.540	0.743	0.953		
4	0.014	0.108	0.222	0.400	0.661	0.857	1.067		
5	0.014	0.099	0.232	0.375	0.565	0.702	0.854	1.010	
6	0.014	0.114	0.229	0.362	0.572	0.727	0.918	1.089	
7	0.014	0.079	0.168	0.295	0.435	0.645	0.838	1.042	
8	0.014	0.060	0.168	0.265	0.370	0.551	0.773	0.976	
9	0.014	0.102	0.210	0.324	0.534	0.743	0.953		
10	0.014	0.102	0.219	0.324	0.537	0.740	0.949		

Run 8609211046

1	0.014	0.086	0.194	0.311	0.387	0.540	0.743	0.946	
2	0.014	0.080	0.182	0.289	0.394	0.556	0.763		

(Continued)

Trap	Streamer Number								
Number	1	2	3	4	5	6	7	8	9

Run 8609211345

1	0.014	0.089	0.159	0.261	0.394	0.565	0.765		
2	0.014	0.092	0.187	0.314	0.422	0.664	0.867	1.070	
3	0.014	0.089	0.175	0.302	0.534	0.767	0.940		
4	0.014	0.108	0.219	0.330	0.432	0.648	0.959		
5	0.014	0.095	0.197	0.292	0.422	0.594	0.753	0.937	
6	0.014	0.064	0.162	0.270	0.384	0.581	0.765	0.969	1.153
7	0.014	0.102	0.210	0.327	0.413	0.591	0.794	0.997	
8	0.014	0.089	0.181	0.276	0.387	0.556	0.673	0.873	
9	0.014	0.102	0.210	0.324	0.537	0.743	0.956		
10	0.014	0.095	0.210	0.318	0.527	0.737	0.940		
11	0.014	0.089	0.191	0.302	0.384	0.635	0.838		
12	0.014	0.105	0.213	0.324	0.438	0.594	0.803	1.105	
13	0.014	0.092	0.175	0.308	0.524	0.788	1.029		
14	0.014	0.099	0.200	0.318	0.470	0.711	0.950		
15	0.014	0.099	0.187	0.308	0.410	0.676	0.904	1.114	
16	0.014	0.076	0.178	0.257	0.346	0.530	0.689	0.845	1.007

Run 860922073

1	0.014	0.095	0.184	0.299	0.407	0.629	0.896		
2	0.014	0.076	0.153	0.245	0.397	0.638	0.842	1.045	
3	0.014	0.086	0.178	0.308	0.521	0.724	0.927		
4	0.014	0.092	0.162	0.305	0.416	0.629	0.838		
5	0.014	0.073	0.206	0.324	0.400	0.562	0.765	1.019	
6	0.014	0.083	0.165	0.276	0.391	0.537	0.708	0.854	1.013
7	0.014	0.105	0.181	0.283	0.429	0.740	0.943	1.121	
8	0.014	0.076	0.191	0.305	0.451	0.648	0.861	1.067	

Run 8609221600

1	0.014	0.095	0.203	0.283	0.397	0.575	0.816		
2	0.014	0.070	0.172	0.286	0.403	0.549	0.759	0.965	
3	0.014	0.083	0.191	0.311	0.470	0.632	0.943		
4	0.014	0.095	0.194	0.321	0.400	0.534	0.743		
5	0.014	0.095	0.203	0.305	0.419	0.584	0.784	0.988	
6	0.014	0.060	0.200	0.318	0.378	0.524	0.702	0.899	1.165
7	0.014	0.089	0.197	0.330	0.457	0.613	0.759	0.965	
8	0.014	0.076	0.165	0.264	0.391	0.537	0.756	0.962	
9	0.014	0.102	0.213	0.327	0.537	0.743	0.940		
10	0.014	0.089	0.178	0.308	0.524	0.734	0.930		

(Continued)

Table A2 (Concluded)

Trap Number	Streamer Number								
	1	2	3	4	5	6	7	8	9
				Run 8609221750					
1	0.014	0.092	0.194	0.289	0.394	0.565	0.743		
2	0.014	0.095	0.187	0.302	0.419	0.549	0.762		
3	0.014	0.083	0.191	0.368	0.534	0.740	1.045		
4	0.014	0.089	0.194	0.318	0.451	0.657	0.861	1.070	
5	0.014	0.102	0.219	0.337	0.438	0.616	0.819	1.067	
6	0.014	0.095	0.191	0.305	0.397	0.559	0.718	0.972	
7	0.014	0.099	0.216	0.337	0.448	0.607	0.756	0.965	1.181
8	0.014	0.095	0.203	0.299	0.422	0.562	0.772	1.077	
9	0.014	0.121	0.216	0.330	0.543	0.753	0.962		
10	0.014	0.089	0.213	0.315	0.524	0.737	0.934		
				Run 8609231035					
1	0.014	0.108	0.219	0.327	0.391	0.594	0.882		
2	0.014	0.080	0.156	0.266	0.406	0.571	0.762	0.964	
3	0.014	0.089	0.207	0.365	0.543	0.746	1.051		
4	0.014	0.096	0.204	0.324	0.432	0.642	0.852		
5	0.014	0.099	0.210	0.324	0.429	0.655	0.855	1.054	

Table A3

Water Levels

Time EDST	Water Level m, NGVD
Run 8609151345	
1342	-0.25
1348	-0.22
1354	-0.20
1400	-0.17
1406	-0.17
1412	-0.14
Run 8609151630	
1630	0.52
1636	0.53
1642	0.55
1648	0.58
1654	0.60
Run 8609181225	
1224	-0.14
1230	-0.16
1236	-0.20
1242	-0.23
1248	-0.27
1254	-0.29
Run 8609181453	
1448	-0.49
1454	-0.49
1500	-0.45
1506	-0.44
1512	-0.46
1518	-0.45
1524	-0.44

(Continued)

A13

Table A3 (Concluded)

<u>Water Levels</u>

Time EDST	Water Level m, NGVD
<u>Run 8609201045</u>	
1042	0.63
1048	0.64
1054	0.63
1100	0.62
1106	0.59
1112	0.56
1118	0.57
1124	0.52
1130	0.50
1136	0.48
<u>Run 8609201500</u>	
1500	-0.40
1506	-0.41
1512	-0.41
1518	-0.43
1524	-0.46
1530	-0.49
1536	-0.45
1542	-0.47
1548	-0.41

A14

Table A4

Horizontal Coordinates of the Photopoles[*]

Pole No.	Offshore Coordinate Distance, m	Longshore Coordinate Distance, m
1	101.3	941.6
2	107.3	941.6
3	112.8	941.9
4	118.5	941.8
5	125.0	941.7
6	131.5	941.5
7	137.4	941.5
8	143.3	941.8
9	148.8	941.6
10	155.0	941.9
11	160.2	942.0
12	166.4	941.8
13	172.0	941.9
14	178.1	941.8
15	184.4	941.8
16	190.0	942.0
17	196.0	942.2
18	202.8	942.4
19	208.0	942.4
20	213.7	942.4
21	219.0	943.0
22	225.5	943.1

[*] From Ebersole and Hughes (in preparation).

Table A5

Grain Size Statistics

Run ID and Trap No.	Streamer No.	Moment Statistics				Folk Inclusive Graphic Statistics				
		First PHI	Second PHI	Third	Fourth	Median PHI	Mean PHI	Standard Deviation PHI	Skewness	Kurtosis
8609111745										
1	1	2.21	0.80	0.00	6.00	2.34	2.32	0.56	-0.22	1.38
3	1	2.56	0.41	-2.07	13.19	2.59	2.60	0.31	-0.10	1.04
4	1	2.55	0.56	-2.67	15.56	2.66	2.62	0.41	0.32	0.71
5	1	2.65	0.46	-2.01	14.13	2.69	2.68	0.34	-0.12	0.99
8609121037										
1	1	2.51	0.43	-1.44	11.52	2.53	2.53	0.30	0.06	0.00
	2	2.58	0.49	-2.40	15.30	2.64	2.62	0.38	-0.16	0.98
	3	2.54	0.48	-2.64	18.31	2.51	2.50	0.36	0.12	0.00
	4	2.60	0.38	-0.73	4.21	2.63	2.62	0.35	-0.11	0.90
	5	2.58	0.42	-2.62	25.35	2.61	2.61	0.34	-0.11	0.88
	6	2.63	0.41	-0.87	4.83	2.68	2.65	0.37	-0.20	0.86
2	1	2.06	0.74	-1.66	7.44	2.15	2.13	0.63	0.17	1.23
	2	2.36	0.52	-1.08	6.26	2.40	2.39	0.46	-0.09	0.95
	3	2.50	0.55	-2.33	15.39	2.55	2.54	0.43	-0.13	0.87
	4	2.63	0.46	-1.67	8.85	2.74	2.66	0.37	-0.42	0.82
	5	2.69	0.42	-0.86	4.42	2.78	2.71	0.36	-0.41	0.81
3	1	2.29	0.48	-1.41	11.28	2.32	2.31	0.43	0.03	1.02
	2	2.39	0.48	-2.03	14.01	2.42	2.42	0.40	-0.03	1.01
	3	2.44	0.48	-2.01	14.31	2.46	2.47	0.40	-0.02	0.97
	4	2.58	0.41	-0.37	3.41	2.60	2.59	0.39	-0.11	0.83
4	1	2.42	0.61	-3.11	18.12	2.50	2.49	0.40	-0.14	1.04
	2	2.69	0.34	-0.88	5.56	2.73	2.71	0.30	-0.21	0.85
	3	2.72	0.36	-1.88	11.16	2.79	2.74	0.30	-0.32	0.82
	4	2.74	0.36	-1.92	12.13	2.79	2.76	0.30	-0.23	0.99
	5	2.68	0.46	-2.59	14.01	2.78	2.73	0.33	-0.36	1.00
5	1	2.72	0.49	-4.99	37.43	2.77	2.77	0.26	0.12	0.96
	2	2.76	0.49	-5.29	42.08	2.03	2.79	0.22	0.35	0.84
	3	2.57	0.68	-2.41	9.81	2.76	2.68	0.51	-0.50	1.76
	4	2.77	0.35	-2.44	16.15	2.82	2.79	0.24	-0.33	0.93
	5	2.82	0.29	-1.32	10.63	2.85	2.82	0.22	-0.33	0.76
	6	2.80	0.27	-0.78	5.32	2.82	2.80	0.23	-0.22	0.83
6	1	2.65	0.41	-3.04	19.75	2.70	2.70	0.27	-0.12	0.96
	2	2.67	0.38	-3.87	32.35	2.70	2.70	0.24	0.05	0.07
	3	2.65	0.61	-3.14	15.43	2.80	2.75	0.38	-0.39	1.35
8609151345										
3	1	1.81	1.23	-1.39	3.72	2.34	1.75	1.21	0.70	1.63
	2	2.47	0.44	-2.26	16.55	2.48	2.51	0.34	0.04	1.05
	3	2.46	0.43	-1.83	11.73	2.40	2.40	0.35	0.07	1.10
	4	2.47	0.52	-3.31	21.57	2.52	2.53	0.34	0.06	1.07
	5	2.50	0.41	-2.76	20.24	2.51	2.53	0.30	0.03	1.14
4	1	2.51	0.64	-3.65	21.82	2.61	2.60	0.39	-0.18	1.24
	2	2.57	0.78	-3.75	18.66	2.73	2.71	0.37	-0.25	1.32

(Continued)

		Moment Statistics				Folk Inclusive Graphic Statistics				
Run ID and Trap No.	Streamer No.	First PHI	Second PHI	Third	Fourth	Median PHI	Mean PHI	Standard Deviation PHI	Skewness	Kurtosis
8609161116										
1	1	2.66	0.52	-3.70	23.73	2.75	2.72	0.31	-0.24	1.00
	2	2.74	0.29	-1.56	18.84	2.76	2.75	0.25	-0.13	0.90
	3	2.74	0.28	-0.72	5.64	2.75	2.75	0.24	-0.13	0.88
	4	2.78	0.32	-2.08	14.62	2.03	2.77	0.25	0.24	0.76
2	1	2.60	0.46	-3.57	32.40	2.64	2.64	0.34	0.13	0.70
	2	2.82	0.27	-0.64	3.95	2.05	2.01	0.22	0.31	0.04
	3	2.85	0.27	-1.14	6.01	2.07	2.05	0.23	0.33	1.03
	4	2.80	0.33	-2.36	15.14	2.84	2.82	0.24	-0.22	0.92
3	1	2.68	0.52	-3.95	26.66	2.76	2.73	0.31	0.23	0.93
	2	2.76	0.32	-0.68	3.96	2.80	2.77	0.30	-0.16	0.89
	3	2.76	0.30	-0.41	3.11	2.79	2.76	0.26	-0.25	0.75
	4	2.67	0.62	-3.09	14.46	2.81	2.76	0.36	-0.39	1.27
4	1	2.29	0.88	-2.61	10.68	2.41	2.44	0.66	0.37	2.00
	2	2.68	0.36	-2.02	17.22	2.70	2.70	0.29	-0.06	0.90
	3	2.71	0.32	-0.46	3.47	2.74	2.72	0.27	0.17	0.82
	4	2.76	0.33	-1.23	7.87	2.81	2.76	0.27	-0.30	0.85
	5	2.71	0.42	-2.70	15.79	2.78	2.74	0.27	-0.29	0.79
	6	2.74	0.47	-2.83	14.26	2.84	2.79	0.31	-0.32	1.07
5	1	2.59	0.34	-0.98	7.81	2.60	2.61	0.29	-0.03	1.01
	2	2.65	0.46	-3.18	22.26	2.71	2.68	0.31	0.22	0.09
	3	2.71	0.38	-2.46	18.98	2.76	2.73	0.27	0.21	0.82
	4	2.73	0.32	-0.78	4.60	2.77	2.74	0.27	-0.28	0.78
	5	2.71	0.42	-3.00	20.02	2.78	2.75	0.29	-0.25	0.82
6	1	2.59	0.38	-0.68	9.32	2.62	2.61	0.34	0.11	0.75
	2	2.60	0.43	-2.29	16.13	2.64	2.63	0.35	0.13	0.94
	3	2.60	0.34	-1.02	9.17	2.62	2.62	0.30	0.07	0.97
	4	2.60	0.34	-0.73	5.32	2.62	2.62	0.31	0.04	0.73
	5	2.68	0.34	-1.16	10.13	2.71	2.68	0.30	0.17	0.05
	6	2.69	0.33	-0.57	3.76	2.73	2.70	0.31	-0.20	0.83
7	1	2.46	0.46	-1.64	11.07	2.41	2.47	0.39	0.00	1.07
	2	2.52	0.40	-1.11	8.11	2.53	2.54	0.35	0.07	1.00
	3	2.46	0.45	-1.90	11.97	2.49	2.48	0.37	0.08	1.17
	4	2.53	0.43	-1.77	13.06	2.56	2.56	0.37	0.12	0.77
	5	2.57	0.40	-1.15	7.32	2.60	2.59	0.36	0.13	0.95
	6	2.57	0.45	-2.57	18.92	2.62	2.61	0.35	0.15	0.95
	7	2.66	0.35	-1.32	12.69	2.70	2.67	0.33	-0.15	0.89
8	1	2.40	0.51	-1.91	10.68	2.47	2.44	0.42	0.20	1.20
	2	2.46	0.50	-1.74	9.81	2.52	2.48	0.42	0.10	1.06
	3	2.46	0.49	-2.51	16.05	2.51	2.49	0.30	0.16	1.13
	4	2.48	0.53	-2.64	16.77	2.54	2.54	0.40	0.11	1.10
	5	2.53	0.40	-0.99	5.62	2.56	2.56	0.36	0.10	1.01
	6	2.53	0.42	-2.27	18.91	2.56	2.56	0.35	0.00	1.12
	7	2.60	0.42	-1.47	8.11	2.65	2.63	0.35	-0.17	0.96

(Continued)

(Sheet 2 of 4)

A17

Run ID and Trap No.	Streamer No.	Moment Statistics				Folk Inclusive Graphic Statistics				
		First PHI	Second PHI	Third	Fourth	Median PHI	Mean PHI	Standard Deviation PHI	Skewness	Kurtosis
8609181453										
5	1	2.60	0.43	-3.56	35.82	2.64	2.63	0.33	0.16	0.94
	2	2.64	0.39	-2.57	20.40	2.67	2.67	0.31	0.06	0.97
	3	2.68	0.34	-1.45	16.35	2.70	2.61	0.30	0.09	0.10
	4	2.66	0.32	-1.61	19.84	2.68	2.68	0.20	0.01	0.94
	5	2.68	0.30	-0.37	3.38	2.69	2.69	0.28	-0.05	0.88
	6	2.74	0.31	-0.83	4.83	2.70	2.75	0.27	0.27	0.03
	7	2.71	0.53	-4.46	31.96	2.81	2.78	0.28	-0.24	1.03
8609191230										
7	1	2.49	0.55	-3.09	18.43	2.57	2.55	0.38	-0.15	1.15
	2	2.55	0.47	-2.49	15.54	2.60	2.59	0.35	0.14	1.04
	3	2.62	0.38	-1.80	13.91	2.64	2.64	0.31	0.13	0.93
	4	2.65	0.33	-0.64	4.06	2.68	2.66	0.30	0.11	0.92
	5	2.62	0.45	-4.35	36.42	2.65	2.65	0.29	0.05	0.96
	6	2.68	0.31	-0.57	4.16	2.69	2.69	0.21	0.01	0.00
8609201045										
1	1	2.52	0.49	-2.30	14.31	2.50	2.57	0.30	0.15	1.02
	2	2.50	0.41	-1.81	12.21	2.52	2.53	0.34	-0.05	1.11
	3	2.46	0.55	-2.70	14.94	2.51	2.52	0.38	-0.11	1.27
	4	2.52	0.44	-2.34	17.60	2.54	2.55	0.35	-0.07	0.91
	5	2.52	0.38	-1.32	9.76	2.52	2.54	0.33	0.02	1.11
	6	2.38	0.75	-2.36	10.30	2.56	2.48	0.60	-0.40	1.54
	7	2.40	0.78	-2.54	10.15	2.59	2.54	0.61	-0.42	2.01
2	1	2.53	0.41	-2.05	15.17	2.53	2.56	0.33	0.02	0.96
	3	2.55	0.50	-3.75	27.81	2.60	2.60	0.34	-0.10	0.96
	4	2.60	0.40	-1.71	10.77	2.65	2.65	0.35	-0.15	0.99
3	1	2.30	0.76	-2.69	11.88	2.45	2.41	0.55	0.31	1.67
	3	2.55	0.46	-3.43	31.06	2.59	2.58	0.35	-0.11	0.99
	4	2.59	0.34	-0.31	3.01	2.59	2.60	0.33	-0.01	0.93
	5	2.45	0.87	-3.51	15.75	2.64	2.60	0.39	-0.24	1.14
	6	2.54	0.39	-0.73	4.02	2.58	2.56	0.37	-0.15	1.03
4	1	2.57	0.51	-3.04	20.51	2.64	2.63	0.36	-0.15	0.99
	2	2.62	0.47	-1.94	7.95	2.70	2.71	0.35	-0.17	1.30
	3	2.67	0.41	-2.87	22.31	2.73	2.70	0.32	-0.19	0.98
	4	2.60	0.55	-3.28	19.67	2.71	2.68	0.36	-0.31	1.21
	5	2.58	0.57	-2.91	16.41	2.70	2.64	0.40	-0.32	1.11
5	1	2.59	0.44	-2.25	14.90	2.65	2.62	0.37	-0.20	1.02
	2	2.62	0.45	-4.70	46.48	2.67	2.65	0.32	-0.16	1.01
	3	2.69	0.33	-0.70	3.49	2.73	2.70	0.31	-0.23	0.94
6	1	2.58	0.35	-0.72	4.33	2.61	2.60	0.32	-0.10	1.02
	2	2.67	0.34	-0.65	3.41	2.71	2.68	0.33	-0.19	0.96
	4	2.62	0.41	-1.92	10.67	2.68	2.66	0.33	-0.22	1.02
7	1	2.68	0.34	-1.69	14.41	2.72	2.70	0.30	-0.16	0.93

(Continued)

Run ID and Trap No.	Streamer No.	Moment Statistics				Folk Inclusive Graphic Statistics				
		First PHI	Second PHI	Third	Fourth	Median PHI	Mean PHI	Standard Deviation PHI	Skewness	Kurtosis
8609201045										
8	1	2.58	0.44	-3.80	31.14	2.61	2.62	0.30	-0.05	1.10
	2	2.54	0.40	-3.14	24.81	2.56	2.59	0.28	0.04	1.20
	3	2.59	0.51	-3.16	19.71	2.65	2.65	0.34	-0.14	1.12
	4	2.69	0.33	-0.71	3.95	2.73	2.71	0.31	-0.15	1.02
	5	2.71	0.32	-0.75	3.81	2.75	2.72	0.30	-0.20	0.98
	6	2.74	0.31	-0.62	3.34	2.78	2.76	0.30	-0.17	1.00
8609201500										
9	1	2.41	0.73	-2.55	11.80	2.55	2.50	0.52	-0.30	1.14
	2	2.67	0.49	-3.05	20.53	2.75	2.71	0.35	0.29	1.00
	3	2.76	0.38	-1.50	10.40	2.84	2.78	0.34	-0.31	0.97
	4	2.81	0.36	-1.12	4.58	2.89	2.83	0.33	-0.33	1.03
10	1	2.58	0.55	-3.06	19.35	2.67	2.64	0.31	0.23	0.91
	2	2.73	0.30	-1.75	13.05	2.77	2.74	0.23	-0.18	0.93
	3	2.86	0.49	-6.23	57.01	2.95	2.88	0.21	-0.60	1.30
	4	2.72	0.53	-3.75	24.66	2.87	2.77	0.33	-0.58	1.20
8609211345										
15	1	2.46	0.87	-2.75	11.36	2.69	2.61	0.61	-0.48	1.77
	3	2.86	0.26	-2.03	11.87	2.92	2.88	0.19	-0.40	1.17
16	1	2.49	0.74	-3.08	16.30	2.65	2.58	0.49	-0.36	1.11
	2	2.73	0.44	-2.14	10.67	2.85	2.75	0.32	-0.56	1.05
	3	2.74	0.60	-3.93	24.29	2.89	2.79	0.32	-0.62	1.25
	4	2.75	0.47	-2.02	8.46	2.89	2.79	0.36	-0.51	1.32
	5	2.86	0.40	-5.17	54.37	2.93	2.86	0.22	-0.54	1.23
8609221600										
1	1	2.72	0.34	-2.88	31.00	2.75	2.74	0.26	0.14	0.00
	2	2.71	0.32	-2.57	33.79	2.72	2.72	0.27	0.09	0.06
	3	2.66	0.42	-3.97	32.39	2.70	2.70	0.28	0.01	0.91
	4	2.66	0.51	-4.32	31.12	2.74	2.72	0.21	0.11	0.92
	5	2.66	0.37	-3.51	33.64	2.61	2.60	0.57	0.09	0.94
	6	2.69	0.41	-3.72	30.97	2.73	2.72	0.27	0.15	0.03
	7	2.75	0.31	-1.68	12.66	2.78	2.76	0.26	-0.20	0.80
2	1	2.84	0.32	-2.60	19.78	2.01	2.04	0.21	0.41	0.95
	2	2.79	0.46	-3.66	23.14	2.01	2.03	0.26	0.47	1.14
	3	2.80	0.37	-4.14	32.81	2.86	2.84	0.21	-0.29	0.97
	4	2.85	0.23	-0.63	5.54	2.87	2.86	0.18	-0.26	0.88
	5	2.86	0.22	-0.35	4.70	2.87	2.86	0.19	-0.11	1.00
	6	2.90	0.41	-4.84	35.31	2.98	2.93	0.19	-0.48	1.26
	7	2.88	0.42	-4.20	28.98	2.97	2.91	0.22	-0.54	1.39
	8	2.61	0.86	-2.39	8.86	2.95	2.71	0.65	-0.76	2.18
8609231035										
2	1	2.45	0.51	-2.98	18.72	2.50	2.50	0.36	-0.09	1.05

APPENDIX B: NOTATION

α	Empirical coefficient
β	Empirical coefficient
c	Empirical coefficient to convert wet weight to dry weight
dH_{rms}/dx	Local cross-shore gradient of wave height
DW	Dry weight of sediment, kg (force)
Δa	Distance between nozzles, m
Δh	Height of streamer nozzle, m
Δt	Sampling time interval, sec
Δw	Width of streamer nozzle, m
F	Sand flux (measured), kg/(m^2-sec)
FE	Sand flux (estimated), kg/(m^2-sec)
g	Acceleration due to gravity, m/sec^2
H	Mean wave height, m
Hmax	Maximum wave height, m
Hmin	Minimum wave height, m
H_{mo}	Spectrally based significant deepwater wave height, m
H_{rms}	Root-mean-square wave height (also Hrms), m
H_s	Significant wave height (also Hs), average of the highest one-third wave heights, m
H10	Average of the highest one-tenth wave heights, m
i	Transport rate density, kg/(m-sec)
k	Streamer number
κ	Empirical coefficient
Kurt(H)	Kurtosis of wave height elevations relative to mean
Kurt(T)	Kurtosis of wave period relative to mean
N	Total number of streamers in a trap
ρ	Density of seawater, kg/m^3
r^2	Squared correlation coefficient
S	Weight of sand, kg (force)
S(H)	Standard deviation in wave height, m
S(T)	Standard deviation in wave period, sec
Skew(H)	Skewness of wave height elevations relative to mean

Skew(T)	Skewness of wave period relative to mean
σ_v	Standard deviation of longshore current speed, m/sec
T	Mean wave period, sec
Tmax	Maximum wave period, sec
Tmin	Minimum wave period, sec
T_p	Spectral peak wave period, sec
Trms	Root-mean-square wave period, sec
Ts	Average of the highest one-third wave periods, sec
T10	Average of the highest one-tenth wave periods, sec
V	Average longshore current speed, m/sec
Var(H)	Variance in wave height relative to mean, m^2
Var(T)	Variance in wave period relative to mean, sec^2
WW	Weight of sediment in drip-free condition, kg (force)
x	Distance offshore, m
y	Distance alongshore, m